Original Research Article

COMPARATIVE ASSESSEMNET OF AQUIFER VULNERABILTY NEAR MAJOR DUMPSITES AROUND KARU-ABUJA AND KEFFI IN NASARAWA STATE, NIGERIA USING INTEGRATED GEOPHYSICAL METHODS

ABSTRACT

This study evaluated the aquifer vulnerability to leachate infiltration near major dumpsites in Karu-Abuja and Keffi in Nasarawa State, Nigeria, using geophysical methods − Vertical Electrical Sounding, 2-D Electrical Resistivity Tomography, Self-Potential and VLF-EM. The study area, located between latitudes 8°56'8.0874"N and 8°56'8.232"N and longitudes 7°40'52.1178"E and 7°40'35.241"E, comprises basement complex and sedimentary rock formations. Nine VES points, four 2-D ERT profiles, ten SP profiles, and sixteen VLF transverses were established at the dumpsites and the control areas. Geophysical data were collected using Ohmega Allied resistivity meter and a Gem VLF receiver, while data interpretation employed tools such as WINRESIST, RES2DINV, GRAPHER, SURFER and KHFFILT. These methods identified groundwater saturation zones and contamination pathways, including fractures and faults. Results identified five to six distinct layers, including Topsoil, clayey sand, weathered/fractured, and fresh bedrocks. Keffi's topsoil resistivity values (47.1-224.2 Ω.m, in depths ≥ 2.1 m) indicate thicker overburden and better aquifer protective layers compared to Karu-Abuja's resistivity values (16.5-294.0 Ω.m, in depths ≥ 0.5 m). Leachate infiltrated zones were identified along four VES points, with low resistivity values ranging from (7.2 to 9.9 Ω.m, in depths ≥ 7.7 m) and (2.8 to 9.6 Ω.m, in depths ≥ 6.37 m) in Karu-Abuja and Keffi respectively. Negative SP anomalies ranging from (– 339.9 to -1.1 mV) and (-135 to -1.65 mV) along the transverses are attributed to electro-kinetic reactions, while high positive VLF current-density ranging from (5 to 10 %) in depths of 14 m are interpreted as electrical conducting paths. The estimated aquifer protective capacity rating for Keffi study area ranged from poor to good with VES 1 (0.043 S), VES 4 (0.05 S), VES 5 (0.01 S) and VES 6 (0.02 S) (approximately 66 %, poor rating), while VES 3 (0.29 S) and VES 4 (0.33 S) (combined 33.33 %, moderate rating); only VES 2 (0.89), representing 16.6 %, indicated good rating. The APC for the Karu-Abuja study area ranged from poor to weak with VES 1 (0.0063 S) and VES 3 (0.002 S), (representing 66.6%, indicating poor rating) and VES 2 (0.1 S) (representing 33.3%, indicating weak rating). This suggests comparatively, that the Keffi study area possess better impervious clay seals to protect groundwater resources against leachate infiltration. Regular Environmental Impact Assessments (EIAs) and the installation of geo-synthetic clay liners at the base of the dumpsites to safeguard groundwater resources from leachate infiltration are therefore recommended.

Keywords: Leachate, aquifer vulnerability, aquifer protective capacity, resistivity, self-potential

1. INTRODUCTION

Aquifer vulnerability measures the protection against contamination and potential water purification from overlying strata, influenced by pollutants from surface sources like leachate,

industrial wastewater, landfill, and chemical fertilizers (Arthur, 2024; Nataraj, 2024). Open dumpsites release such pollutants through slow, anaerobic decomposition, generating leachate, landfill gas, heavy metals, and hazardous pollutants (Koliyabandara *et al.* 2024; Abdel-Shafy *et al*. 2024). These substances seep into underground aquifers via advection, molecular diffusion, mechanical dispersion, and adsorption mechanisms (Wei *et al.* 2024). Groundwater is considered a more sustainable source of potable water than surface water. This is because groundwater undergoes filtering through soil and rock formations, eliminating contaminants like sediments and micro-organisms (Udosen *et al.* 2024). Groundwater is protected by natural barriers like shale, but areas with thin/permeable overburden layers, where aquifers are hydraulically connected to the ground, may be susceptible to surface pollution (Servin Vega, 2024). The filtering capacity of soil and rock is influenced by the composition and rock mineralogy. For instance, sewage is filtered at 30-45 meters during percolation, passing through sandy loam and organic humus. The filtering process involves the decomposition and ion absorption of humus and argillitic minerals. Highly fractured granitic/limestone rocks, due to their permeable nature, are unable to purify sewage at deep travel depths due to rapid fluid/material flow (Udosen *et al.* 2024). Sustainable management of groundwater resources such as the prediction of vulnerability and the protection of groundwater resources are therefore crucial in meeting water supply needs (Huang *et al.* 2024). Groundwater contamination can be managed and minimized by delineating and monitoring vulnerable areas. This study therefore aims to integrate geophysical methods to evaluate and compare aquifer vulnerability, estimate protective capacities, delineate leachate infiltration, and determine groundwater occurrence factors in Karu-Abuja and Keffi with a view to providing a comprehensive guide for policy formulation regarding waste disposal design and siting of water projects. Previous studies have evaluated the aquifer hydraulic properties and groundwater protective capacity in Abavo area, Nigeria (Chinyem and Ovwamuedo, 2024). Results from the pumping test analysis, using the Cooper Jacob's method, revealed that the transmissivity, specific capacity, storativity and hydraulic conductivity are 5.9 m^2/day, 33.13 m/day, 0.0069 and 0.1722 m/day respectively. The study revealed longitudinal conductance and transverse resistance range of 0.001048-0.027828 Ω^{-1} and 105470.4-1255775.3 $\Omega \cdot m^2$ respectively. The study established that the aquifer is semi-confined, has poor protective capacity and high rechargibility. In another study, Chinyem (2024) determined aquifer parameters and groundwater protective capacity in parts of the Nsukwa clan using geoelectric and pumping test methods. The computed *T* and *K* from geoelectric sounding ranged from 11.37 to 34.79 m^2/day, with a mean value of 18.51 m^2/day and 0.8243 m/day, respectively, while the *T* and *K* values from the pumping test are 18.58 m^2/day and 0.8251 m/day, respectively. *S* and *R* values ranged from 0.001179 to 0.0131619 Ω^{-1} and 2434 to 102,090 Ωm^2, respectively, revealing a poor aquifer protective capacity and moderate yield. Also, Satheeshkumar (2024) employed VES method to assess the groundwater potential of Naraiyur micro-watershed. Groundwater potential was observed at point 1. Aquifer capacity in the study area indicates low vulnerability area. Ishola (2024) employed twenty-seven (27) VES to evaluate aquifer protective capacity at Obafemi-Owode LGA, Ogun State South-West Nigeria. Results revealed that the reflection coefficient ranged between 0.02 and 0.98 while protective capacity ranged between 0.00135 and 0.510. A group of researchers probed sixteen VES stations to address potable water challenge in Shango, North-Central Nigeria (Ejepu *et al.* 2024). The result revealed that the hydraulic conductivity ranged from 0.465 to 0.534 m/day, while transmissivity varied from

9.589 m^2/day to 26.029 m^2/day across different VES points. They concluded that regions exhibiting thick layers and low resistivity values indicate high longitudinal conductivity. Another group of researchers employed VES and 2-D ERT surveys, constrained by well lithological information, to investigate leachate infiltration at a major open dump in Eket, Southern Nigeria (Udosen *et al.* 2024). Dar-Zarrouk indices and electrical reflection co-efficient indicated that the highly heterogenous region had moderate aquifer protective capacity and moderate aquifer potentiality.

1.1 LOCATION AND GEOLOGY

The thirty-year old Karu dumpsite and its control centre are situated between latitude ($9^0$0'27.7986"**N** and $9^0$0'45.2016"**N**) and longitude ($7^0$34'23.0982"Eand $7^0$34'23.4006"E), while the Keffi dumpsite and its control centre are situated between latitude (8°50’16.7994"N and 8°50’38.4822"N) and longitudes (7°53’15.36"E and 7°53’2.5002"E). Karu-Abuja and Keffi are underlain by the Basement Complex Rocks of Nigeria, which consists of the migmatite gneisses, the schist belts, the Older Granites suite comprising mainly different varieties of granitic rocks, including charnockites (hypersthene granites), syenites, as well as minor gabbroic and dioritic rocks, and the undeformed acid and basic dykes (Dada, 2006). It forms part of the north-central Basement Complex of Nigeria which comprises Archean and Proterozoic rocks, bearing the imprints of the Liberian (2700 + 200Ma), Eburnean (2000 + 200Ma) and Pan African (600Ma) orogenic events (Oversby, 1975). The main lithologic units identified on a regional scale include; gneiss, schist, pegmatites with well delineated geologic boundaries (Dada, 2006). These rocks have undergone polycyclic deformation, thereby causing the formation of both micro and macro structures. The general structures include joints, foliations, and faults (Dada, 2006). They generally have NNE-SSW trending gneissose foliations with few ENE-WSW and NNW-SSE trends and dip values which vary from as low as 6° to as high as 60° in the S-E directions (Tanko *et al*., 2015). The drainage pattern in the area is dendritic and this reflects a resistance to erosion by the underlying rock units. The drainage features in the area are made up of several streams along channels which drain into the S-E Trending River Uke (Bashir, 2018). The study areas are influenced by two major climatic conditions, the rainy seasons begin in April and peaks in August through October and the dry season from February to early-mid April. The annual rainfall is 1357 mm. The harmattan (dry and dusty wind) experienced from November - January also characterises the dry season. Temperatures range from 26.58^0 to 32.51^0C. High temperatures are usually experienced from February through April to May, while average temperature value is about 26.78^0C from July to September during the rainy season. The area records its highest temperature of about 34^0C during the dry season, which occurs from November to March. During the rainy season April to October, the maximum temperature drops to about 24^0C due to the dense cloud cover (McCurry, 1985). The annual total rainfall is in the range of 1100 mm to 1600 mm (Ajibade and Wright, 1988) shown in Figures 1 and 2.

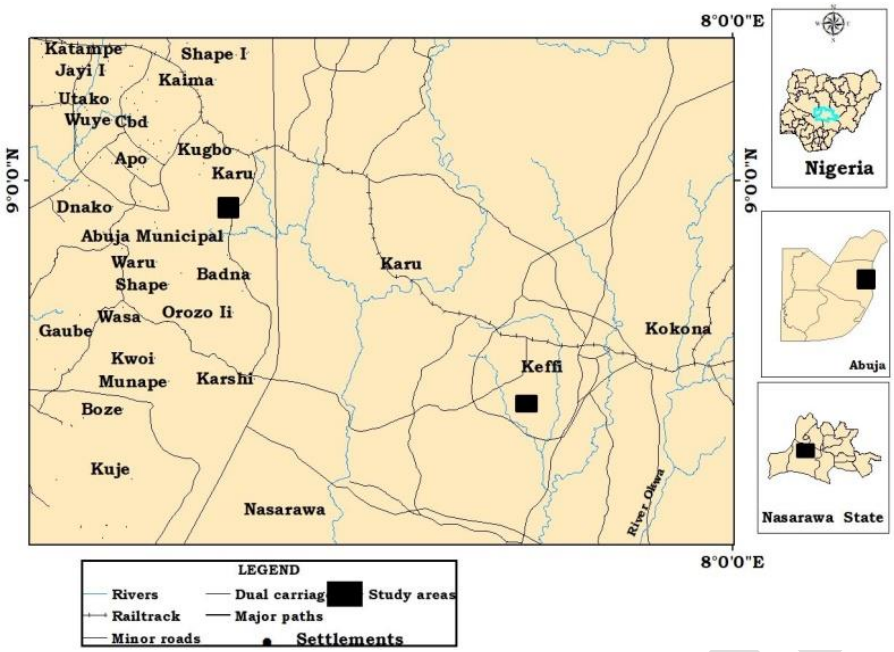

Figure 1: Location map of the study areas (after NASRDA, 2018).

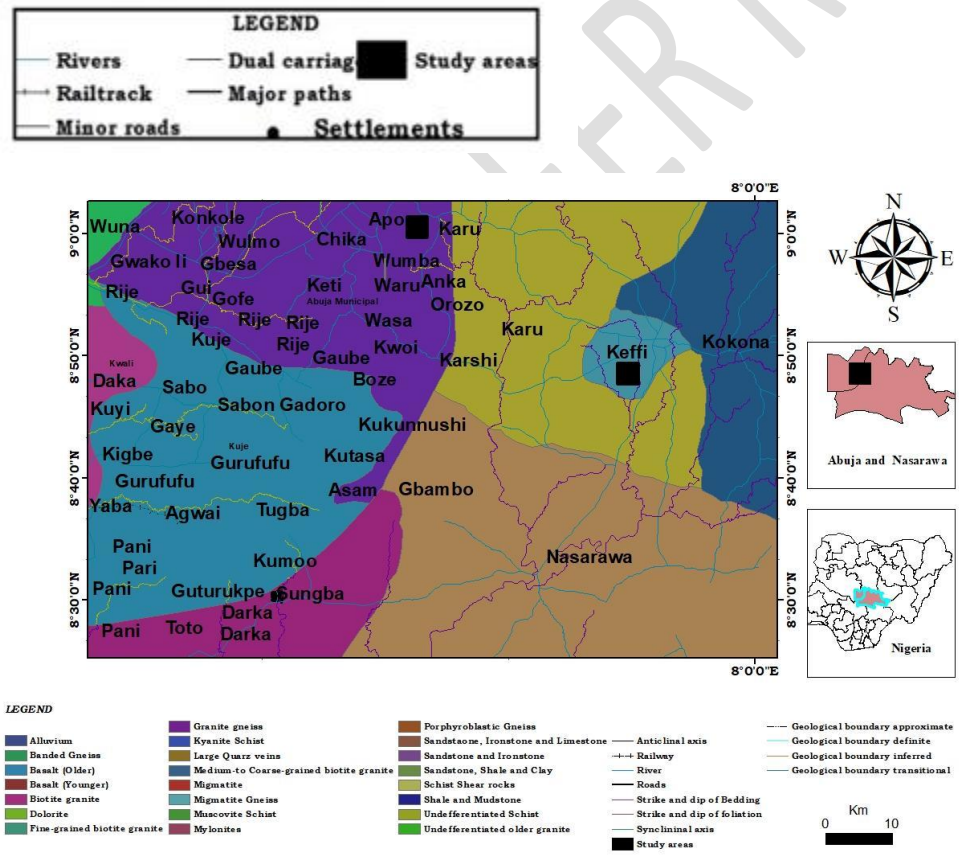

Figure 2: Geological map of the study areas (after NGSA, 2011)

2. MATERIALS AND METHODS

The Ohmega Allied resistivity metre and its accessories, hammer, electrodes/non-polarizable, measuring tape, cables, reels, Global Positioning System (GPS) and a portable GEM VLF receiver were used to obtain VES, 2-D ERT, SP and VLF-EM data. Nine (9) VES points with maximum current electrode spacing (AB/2) of 170 m using Schlumberger array configuration, four (4) 2-D ERT profiles at constant electrode spacing of 5 to 120 m using Wenner array configuration, nine (9) SP profiles at constant electrode spacing of 5 to 170 m, and sixteen (16) VLF-EM profiles at 5 m intervals and a maximum spacing of 100 m, were established at the dumpsite. The VLF-EM data was collected using a portable GEM VLF receiver within the frequency range of 15.1 – 24.0 kHz. Data were also collected at the control centre located about 700 m away from the dumpsite by constraining each of the method along the same transverse. Data collected were interpreted using tools such as WINRESIST, RES2DINV, GRAPHER, SURFER and KHFILT. KHFILT was utilized for filtering and mapping current densities.

2.1 Photographs from the field

a)

b)

Plate 1: Data collection at the Karu-Abuja dumpsite and its control centre

d)

e)

Plate 2: Data collection at the Keffi dumpsite and its control centre

3. RESULTS AND DISCUSSIONS

3.1 Keffi Dumpsite, Panteka Area, Nasarawa State

The summary of results for the six (6) VES points conducted near the Keffi dumpsite and its control centre indicating the No. of layers, Curve Types, resistivity values (Ω.m), thicknesses (m), depth (m) and delineated lithological units are presented in Table 1:

Table 1: Vertical Electrical Sounding data for VES stations 1-6 (Keffi)

VES	No. of Layer (s)	Curve Types	Res. (Ω.m)	Thickness	Depth	Lithological Units
1	5	HA	47.1	0.5	0.5	Topsoil (lateritic)
			9.6	4.1	4.6	Sandy clay, leachate
			116.4	5.0	9.6	Weathered basement (Medium grain sandstone)
			3061.4	42.8	52.4	Partial fresh Basement
			3144.9	-		Fresh Basement
2	5	QA	199.5	1.1	1.1	Topsoil (lateritic)
			12.8	0.6	1.7	Silty Sandy
			2.8	2.5	4.1	leachate
			1257.6	19.2	23.4	Partial fresh Basement
			3586.2	-		Fresh Basement
3	5	HA	224.2	0.8	0.8	Topsoil (lateritic)
			66.8	19.5	20.2	Sandy-clay
			1043.9	16.7	36.9	Partial fresh Basement
			6696	-		Fresh Basement
4	5	HK	113.5	2.1	2.1	Topsoil
			18.9	6.2	8.3	Sandy clay
			3371.3	19.7	28	Partial fresh Basement
			13402.7	-		Fresh Basement
5	5	HA	230.6	1.6	1.6	Topsoil (lateritic)
			78.1	26.1	27.7	Weathered basement (Medium grained sandstone)
			364.9	18	45.7	Fractured basement (Fine grained sand)
			2985.9	-		Fresh Basement
6	5	HK	125.0	1.6	1.6	Topsoil
			9.2	2.6	4.2	Sandy clay
			195.9	3.5	7.7	Weathered/fractured basement (Medium to fine grained sand)
			5384.7	35	42.7	Fresh Basement
			9152	-		Partial fresh Basement

3.2 Estimated Aquifer Parameters of the surveyed area (Keffi)

The primary aquifer parameters (resistivity and thickness) are determined from Table 1 and used to estimate the geo-hydraulic parameters (Table 2). The summary of the Daz-Zarrouk parameters estimated for the weathered aquifers within Keffi dumpsite and its control centre showing the VES points, resistivity values ρ (Ω.m), Aquifer thicknesses h (m), Electrical conductivity σ ($\Omega.m^{-1}$), Longitudinal Conductance S (mhos), Transverse Resistance T_R ($\Omega.m^{-2}$), Hydraulic conductivity K (m/day), Transmissivity T (m^2/day), Quantity of water (Q) and porosity ϕ (%) are presented in Tables 2 and 3:

Table 2: The summary of Dar-Zarrouk parameters and electrical conductivity K (m/day) estimated for the weathered aquifers in the study area (Keffi)

VES	ρ (Ω.m)	Thickness (h/m)	$\sigma = 1/\rho$ ($\Omega.m^{-1}$)	$S = \sigma h$ (mhos)	$T_R = h\rho$ ($\Omega.m^{-2}$)	K (m/day)
1	116.4	5.0	0.0086	0.0430	582.0	4.57
2	2.8	2.5	0.35714	0.8929	7.0	147.88
3	66.8	19.5	0.0150	0.2920	1302.6	7.67
4	18.9	6.2	0.0530	0.3280	117.2	24.91
5	364.9	18.0	0.0027	0.0493	6568.2	1.57
6	195.9	3.5	0.0051	0.0179	685.7	2.81

Table 3: The summary of aquifer transmissivity (T), quantity of water Q and porosity ϕ (%) estimated for the weathered aquifers in the study area (Keffi)

VES	$T = kh$ (m^2/day)	Quantity $Q = (k\sigma)$	Porosity ϕ (%)
1	22.85	0.04	32.34
2	369.70	52.82	47.98
3	149.58	0.115	34.67
4	154.42	1.32	39.97
5	28.33	0.004	27.54
6	9.84	0.014	30.15

3.2.1 Results of computer modeled curve for six (6) VES points (Keffi)

The results of the computer modeled curves for the six (6) VES points conducted within the study area are shown in Figures 9 to 14:

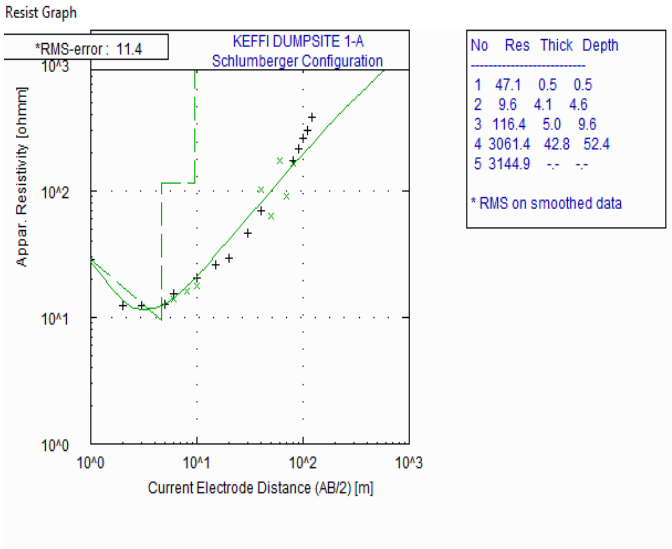

Figure 3: Results of computer modeled curve for VES 1

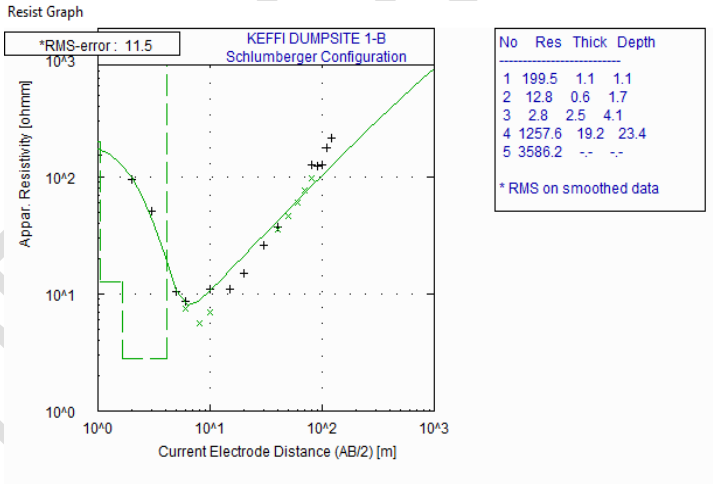

Figure 4: Results of computer modeled curve for VES 2

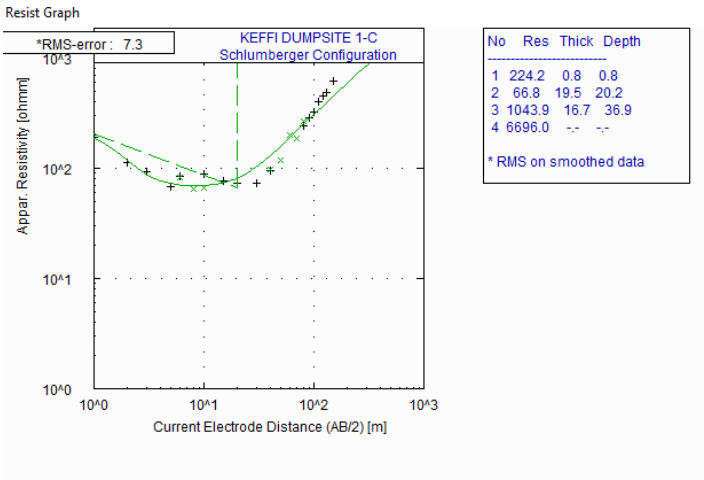

Figure 5: Results of computer modeled curve for VES 3

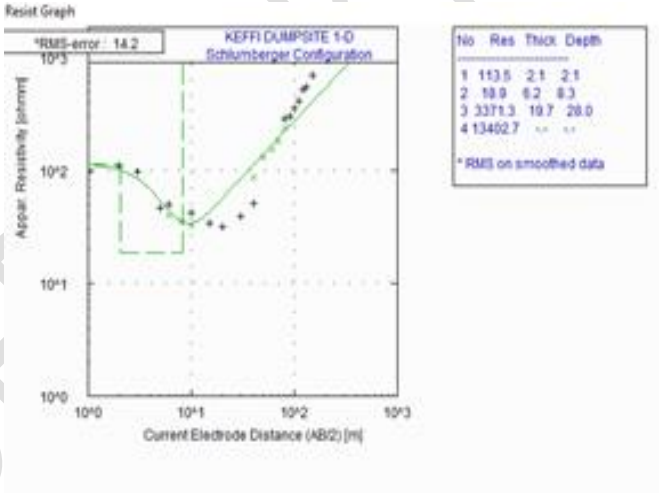

Figure 6: Results of computer modeled curve for VES 4

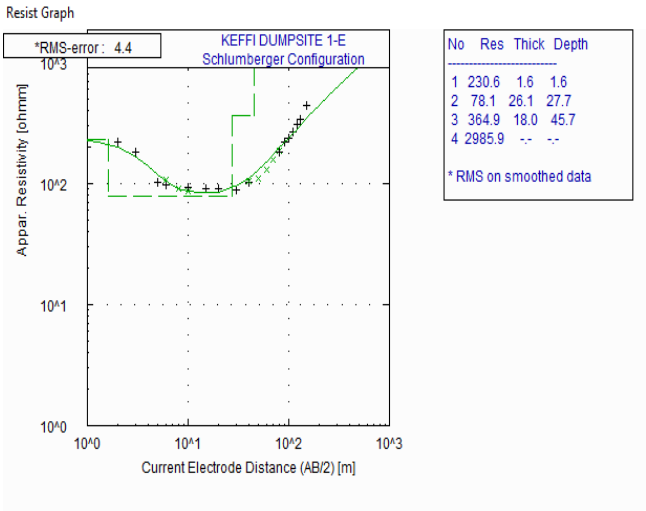

Figure 7: Results of computer modeled curve for VES 5

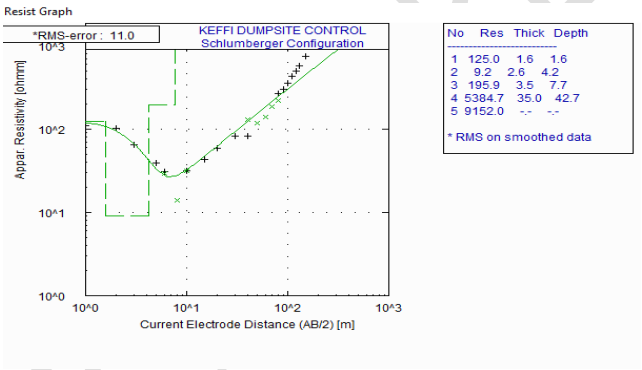

Figure 8: Results of computer modeled curve for VES 6 (Control Centre)

3.2.2 Correlation of Borehole log with VES (Keffi)

The correlation of borehole lithological logs BH (D) and BH (C) with resistivity sounding (VES) results for VES 1-5 and VES 6 (Control Centre) in the study area are shown in Figure 9:

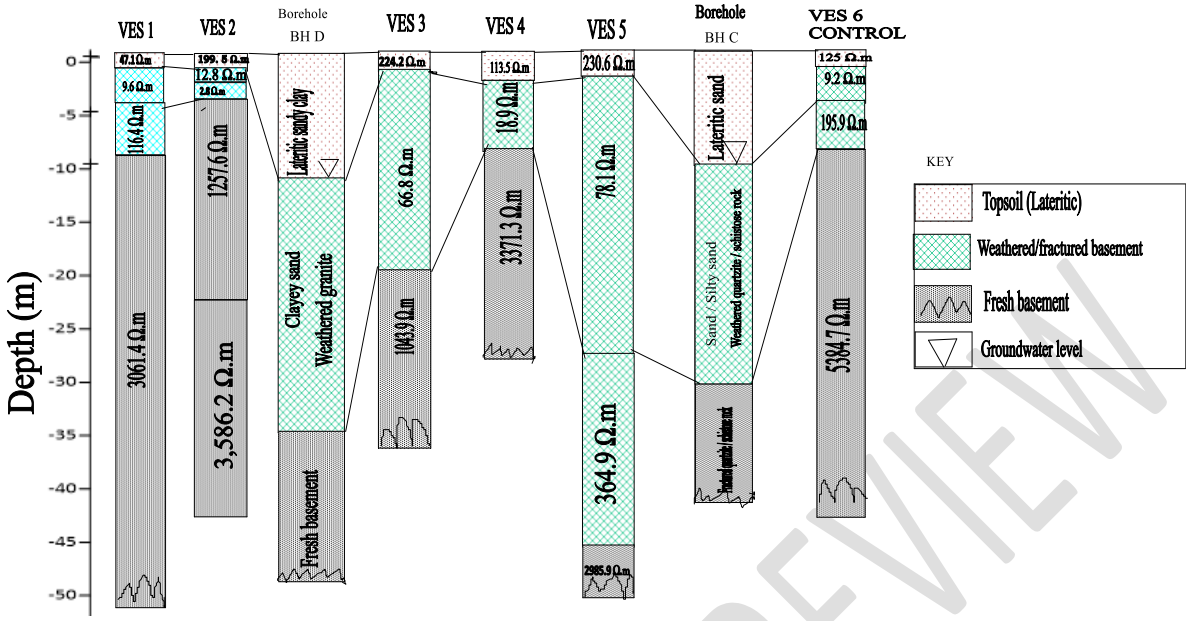

Figure 9: Correlation of resistivity sounding (VES) results with borehole lithological logs in the study area (Keffi)

3.3 Discussion

The study area is characterised by heterogeneous lithology with resistivity values varying from low to high as displayed in the corresponding resistivity-depth profiles in Figures 3 to 8. The geo-electric sections revealed four to five discrete geo-electric layers, consisting of Topsoil (lateritic); second layer interpreted as weathered zone (clayey sand); the third layer inferred as fractured bedrock, while the fourth and fifth layers were interpreted as fresh bedrocks. The identified curve types include: HA (50%), HK (33.3%), QA (16.7%). The HK type was identified at the Control Centre.

3.3.1 The Topsoil

Resistivity values for Topsoil layers and their corresponding thicknesses varies from VES 1 (47.1 to 9.6 Ω m), (0.5 to 4.1 m), VES 2 (199.5 to 12.8 Ω m), (1.1 to 1.7 m), VES 3 (224.2 to 66.8 Ω m), (0.8 to 19.5 m) VES 4 (113.5 to 18.9 Ω m), (2.1 to 6.2 m) VES 5 (230.6 to 78.1 Ω.m), (1.6 to 26.1 m) and VES 6 (Control Centre) (125.0 to 9.2 Ω m), (1.6 to 2.6). This is suggestive of three zones: the belt of the soil water at the top, the intermediate vadose zone, and the capillary fringe at the bottom which acts as the passage for the flow of surface water to the fractured layer known as the zone of aeration.

3.3.2 The Second layer

The resistivity values of the second layer and their corresponding thicknesses varies from VES 1 (9.6 to 116.4 Ω.m), (4.1 to 5.0 m); VES 2 (12.8 to 2.8 Ω m), (0.6 to 2.5); VES 3 (66.8 to 1,043.9 Ω.m), (19.5 to 16.7 m); VES 4 (18.9 to 3371.3 Ω.m), (6.2 to 19.7 m); VES 5 (78.1 to 364.9 Ω.m), (26.1 to 18.0 m) and VES 6 (9.2 to 195.9 Ω.m), (2.6 to 3.5 m). This layer is mostly composed of

weathered to fractured basement, clay, and limestone, in agreement with the geology of the area. This layer consists of priority targets for groundwater exploration.

3.3.3 The third layer

The resistivity values for third layers and their corresponding thicknesses varies from VES 1 (116.4 to 3061.4 Ω.m), (5.0 to 42.8 m), VES 2 (2.8 to 1257.6 Ω.m), (2.5 to 19.2 m), VES 3 (1043.9 to 6696.0 Ω.m), (16.7 to infinity), VES 4 (3,371.3 to 13,402.7 Ω.m), (19.7 to infinity), VES 5 (364.9 to 2,985 Ω.m), (18.0 m to infinity), VES 6 (5,384.7 to 9,152.0 Ω.m), (35.0 m to infinity). This is likely composed of clay, weathered/fractured basement to fresh basement.

3.4 The conductive layers

Conductive layers with resistivity values (> 6.83 Ω.m) were delineated as leachate infiltrated and soil-contaminated zones. The study showed that leachate has spread along transverse 2 and parts of transverse 1, which occurs at a maximum depth of 9.26 m and an average depth of 6.38 m. This was correlated by the 2-D ERT real inverse models.

3.5 Estimated Aquifer Protective Capacity (APC) for the Keffi Study Area

The calculated Longitudinal Conductance S (Table 2) for the study area revealed that the aquifer protective capacity is rated as poor to good with four VES points (VES 1 (0.043 S), VES 4 (0.05 S), VES 5 (0.01 S) and VES 6 (0.02 S)) representing 66% of the sounding points, indicating poor protective capacity rating; two VES points (VES 3 (0.29 S) and VES 4 (0.33 S)) representing 33.33% of the soundings, showed moderate protective capacity rating, while only VES 2 (0.89), representing 16.6% of the soundings, showed good protective capacity. The aquifer protective rating of VES points indicating poor protective capacity (66 %), suggests that the study area is not suitable for the establishment of a landfill, as there are no sufficient impervious clay seals to protect groundwater resources against leachate infiltration.

3.6 Delineation of aquifer systems

Two borehole logs (after Anudu *et al*. 2021) were used to correlate with VES points along the profiles. Borehole log (BH D) was used to infer the lithologic sections derived from the interpretations of VES profiles (1 to 5) around the dumpsite, while Borehole log (BH C) was used to correlate the VES point for the control centre with a view to delineating the aquifer systems in the area (Fig. 9).

3.7 Results of the Self-Potential (SP) survey conducted in the study area (Keffi)

The results of the six (6) SP profiles conducted in the study area are shown in Table 4:

Table 4: Summerised results from self-potential (SP) survey in the study area

Distance X (m)	SP (mV) LINE 1	SP (mV) LINE 2	SP (mV) LINE 3	SP (mV) LINE 4	SP (mV) LINE 5	SP (mV) Control Centre6
0	-28.28	42.83	-69.06	25.51	-1.65	43.44
5	-8.32	-16.49	-75.62	21.81	-50.82	-48.98
10	-135.2	-61.89	-75.59	-49.39	-54.71	70.16
15	-103.4	-17.52	-5.08	5.164	-39.04	29.10

20	-70.08	2.79	-33.40	20.18	-73.36	3.54
25	-56.97	5.41	-57.58	19.57	467.2	-7.81
30	-79.72	92.42	-33.61	-4.447	-50.21	-14.75
35	-68.65	24.69	-54.92	-19.67	-44.26	-54.30
40	-69.47	48.36	-24.59	6.496	-29.71	1.578
45	-79.49	67.01	-23.87	31.15	-19.26	-42.83
50	-50.0	89.14	-50.82	40.57	-40.16	-53.69
55	-42.21	90.78	-93.24	66.4	-5.533	14.55
60	-23.87	91.81	-90.31	36.47	-40.16	-37.60
65	-18.85	47.13	-85.45	81.15	-28.69	-106.50
70	8.238	55.02	-22.74	9.191	-12.09	51.23
75	-14.34	68.04	-13.52	45.49	-10.96	-21.62
80	-39.24	36.17	9.04	-7.89	21.10	-13.52
85	-73.36	32.99	60.86	48.77	-46.93	57.38
90	-44.88	23.67	-24.18	43.03	-6.435	-58.81
95	-64.55	42.62	-39.96	21.51	-61.27	-79.72
100	-40.57	45.29	-1.25	-1.086	-22.33	7.623
105	1.793	45.90	-26.33	-13.01	-15.78	2.22
110	-7.623	39.34	-46.93	-7.582	-43.65	26.12
115	-24.79	84.84	-22.33	-3.463	-84.43	44.67
120	-	-	-37.91	-33.3	-80.74	85.05
125	-	-	-64.35	-3.77	-256.5	-41.10
130	-	-	-68.44	-54.51	-54.92	-3.86
135	-	-	-43.03	-	-60.86	121.90
140	-	-	-83.00	-	-43.85	85.66
145	-	-	-43.85	-	-46.52	49.80

3.8 CORRELATION ANALYSIS

The following cross-sections correlates the Self Potential (mV) profiles, their corresponding SP contours and 3-D SP plots, VES transverses and 2-D ERT geo-electric sections along the survey lines (Figures 10 – 15):

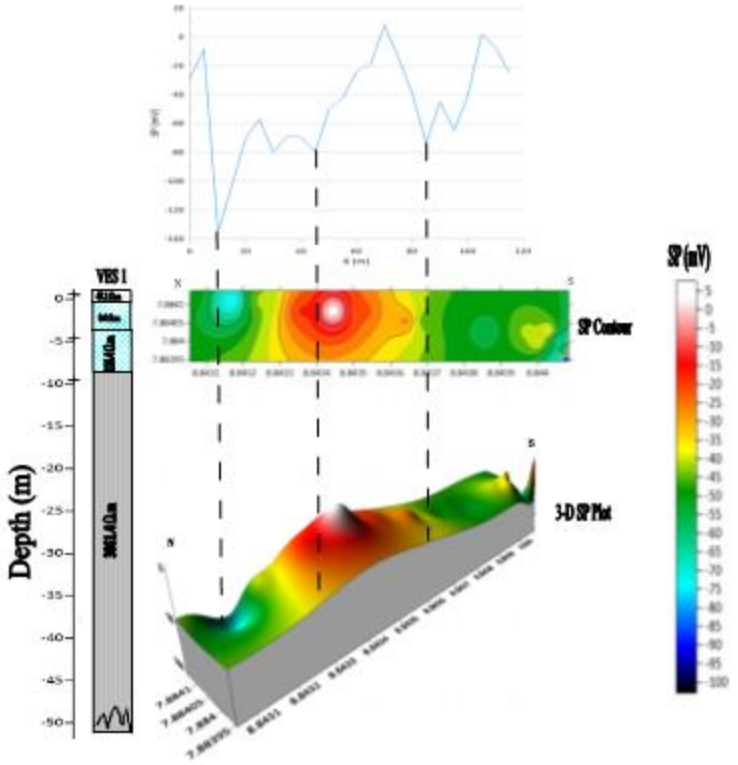

Figure 10: Cross-section correlating the VES transverse, SP signals, SP contours and 3-D SP plot and VES log along Profile 1(Keffi)

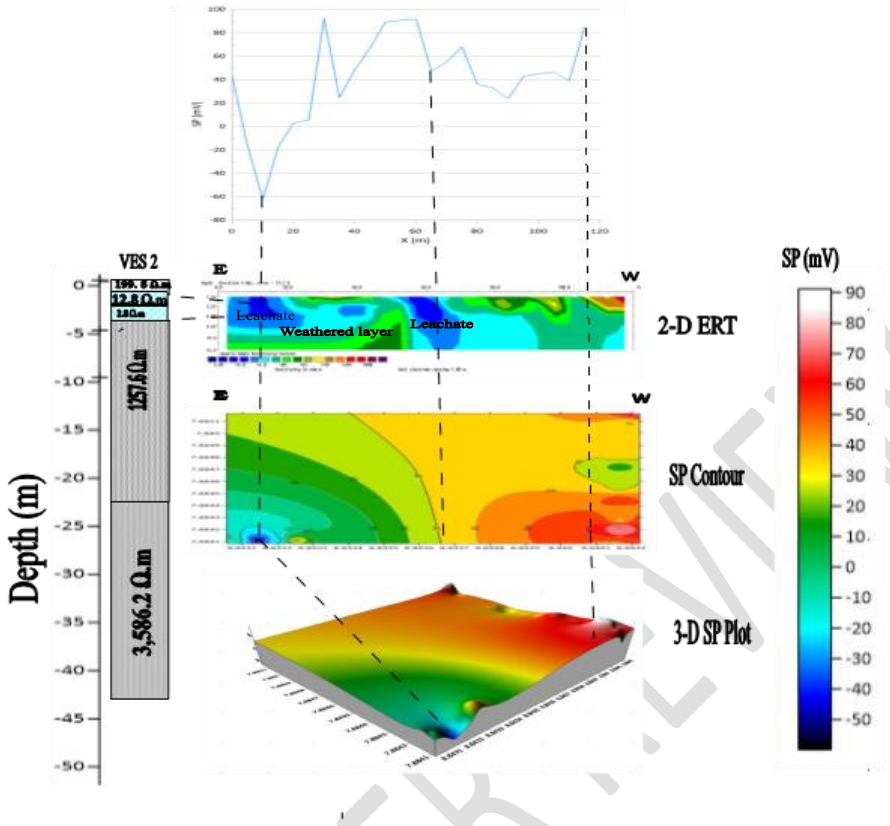

Figure 11: Cross-section correlating the 2-D ERT geo-electric section, VES transverse, Self-Potential signal, SP contour and 3-D SP plot along profile 2(Keffi)

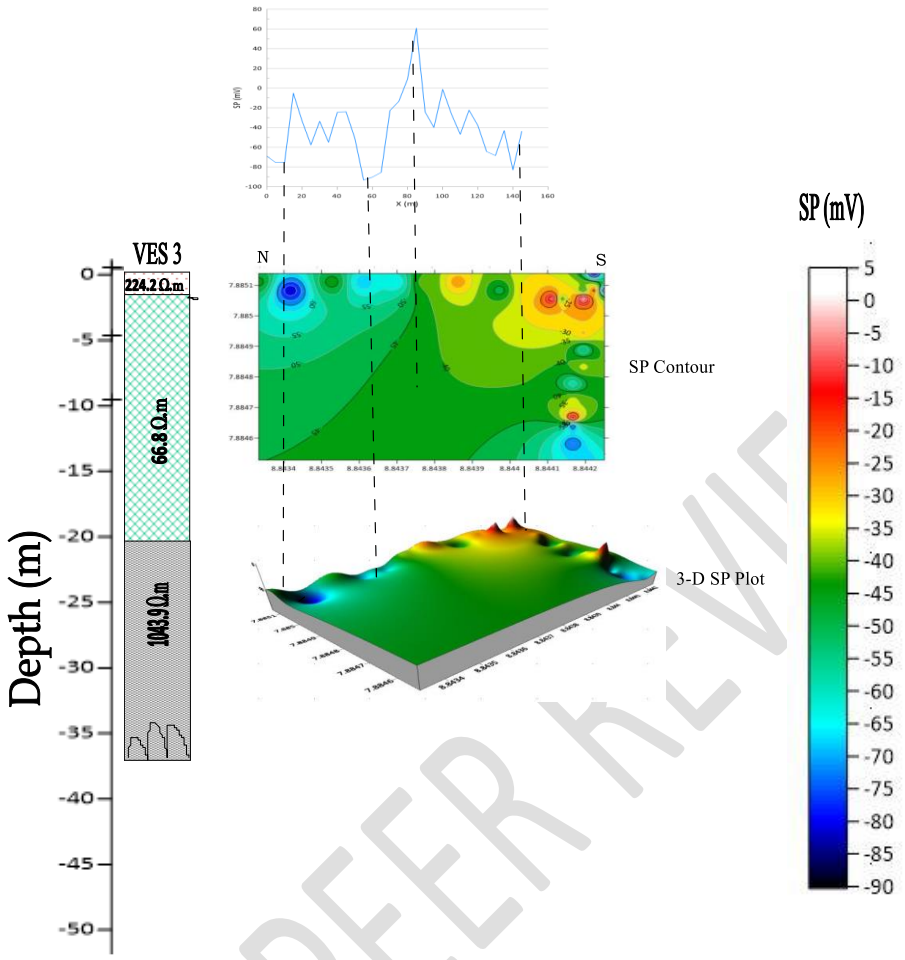

Figure 12: Cross-section correlating the VES transverse, Self-Potential signal, SP contours and 3-D SP plot along Profile 3 (Keffi)

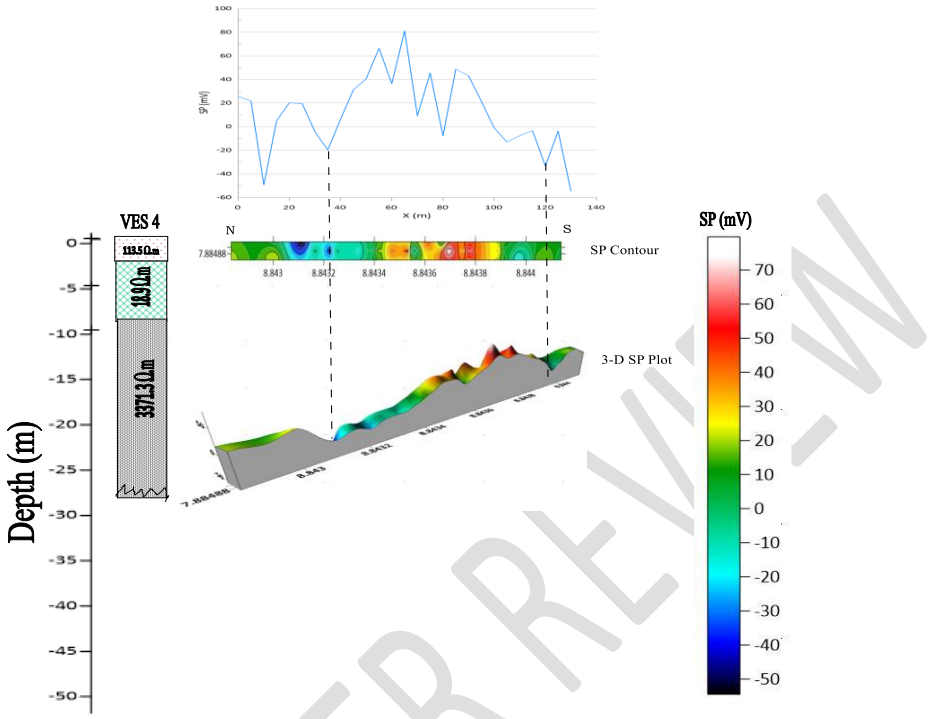

Figure 13: Cross-section correlating the VES transverse, Self-Potential signal, SP contours and 3-D SP plot along Profile 4 (Keffi)

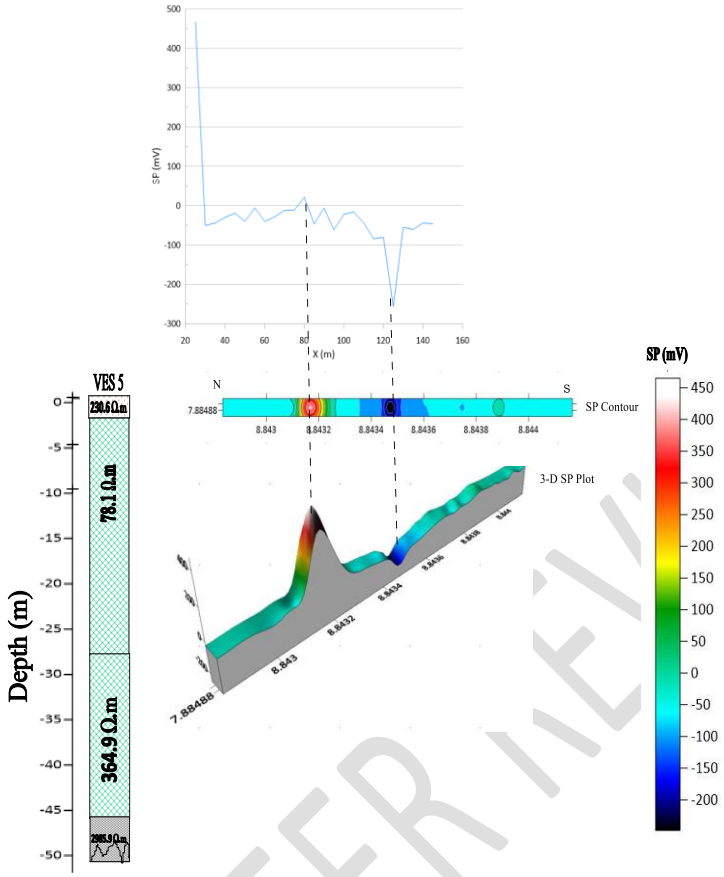

Figure 14: Cross-section correlating the VES transverse, Self-Potential signal, SP contours and 3-D SP plot along Profile 5 (Keffi)

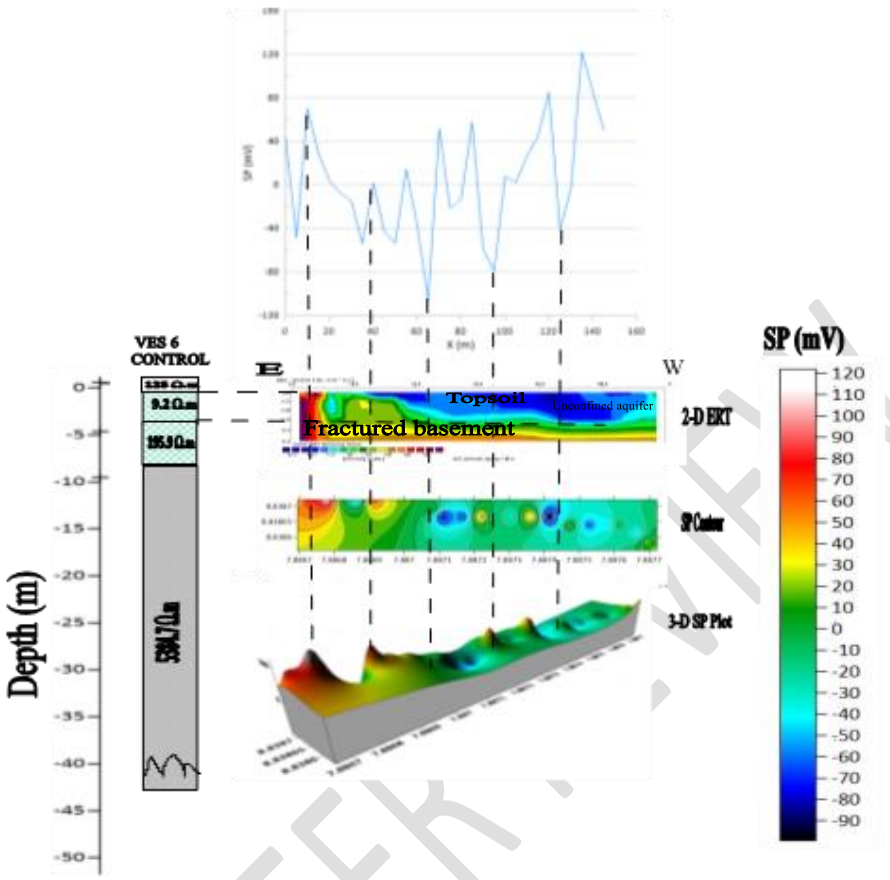

Figure 15: Cross-section correlating the 2-D ERT geo-electric section, VES transverse, Self-Potential profile, SP contour and 3-D SP plot along profile 6 (Keffi)

3.9 Discussion

3.10 Profile 1

The SP anomalies along profile 1 (Figure 10) indicate dominant negative SP distribution patterns ranging from (-100 to -5 mV) between (0 – 120 m) along the survey line. Between (0 to 10 m) is a sharp deviation of the SP anomaly ranging from (-80 to -60 mV) attributed to leachate induced electro-kinetic process flowing in the S-N direction. This correlates with the VES results indicating the presence of materials with low resistivity value of (9.6 Ω.m, to depths ≥ 10 m) along the same transverse, suggestive of leachate infiltrated zone.

3.11 Profile 2

This cross-section (Figure 11) correlates the 2-D ERT, SP contours, 3-D SP plot and SP (in mV) profile 2. The 2-D ERT delineated three (3) geo-electric sections. Stretching from the eastern to the western flank are materials with resistivity values ranging from (53 to 412 Ω.m, to depths ≥ 3.73 m). This was inferred as the topsoil. From the eastern flank are objects with resistivity values ranging from (6.83 to 19.3 Ω.m, to depths ≥ 6.38 m), along (0 to 20 m) interpreted as leachate contaminants flowing in the E-W direction. This result was correlated by the VES log showing objects with low resistivity materials ranging from (2.8 to 12.8 Ω.m, at depths ≥ 8.5 m). Situated

between (50 to 70 m) at the central part of the profile, is a protruded conic-shaped object with resistivity values ranging from (6.83 to 10 Ω.m). This was also interpreted as leachate plume intrusion. At the western flank, spanning between (70 to 90 m) along the survey line, are materials with resistivity values ranging from (53 to 412 Ω.m) interpreted as weathered/fractured bedrock. Between (90 to 120 m) are materials with resistivity values ranging from (1147 to 8996 Ω.m, to depths ≥ 9.26 m) are materials interpreted as fresh basement. This result is correlated by the presence of materials with negative SP anomalies ranging from (- 50 to -10 mV), situated between (10 – 16 m) along the survey line, suggestive of leachate infiltrated contaminants. The 3-D SP contour map also depicts the E-W direction of leachate flow which is closely related to the topographic conditions of the study area. The positive SP anomalies are interpreted as quartz veins in agreement with the geology of the area.

3.11.1 Profile 3

This cross-section (Figure 12) compares the VES Log, SP contours and 3-D SP plot for profile 3. The dominant materials with negative SP values ranging from (-90 to -5 mV) located between (0 – 160 m) along the survey line, is attributed to groundwater streaming potential. This was correlated with the VES results which shows presence of materials with higher resistivity values ranging from (66.8 to 224.2 Ω.m, to depths ≥ 20 m), along the survey line, suggestive of saturated fractured zone. The absence of materials with low resistivity values along the survey line established that the zone is free from leachate contamination due to the distance of the transverse which is 150 m away from the dumpsite.

3.11.2 Profile 4

This cross-section (Figure 13) compares the VES Log, SP profile, SP contours and 3-D SP plot for profile 4. The SP values indicate a variation of positive and negative SP distribution patterns ranging from (-50 to 70 mV) between (0 – 140 m). This is attributed to fluid streaming potential. The VES results with resistivity values ranging from (18.8 to 113.5 Ω.m, to depths ≥ 20 m) is diagnosed as aquifer material hosting groundwater resources. The survey line's distance from the dumpsite, which is 250 meters, indicates that the low resistivity values are not due to the presence of leachate contaminants.

3.11.3 Profile 5

This cross-section (Figure 14) compares the VES Log, SP profile, SP contours and 3-D SP plot for profile 5. The contour map of the self-potential showing variation of positive and negative values ranging from (-200 to 450 mV) is attributed to streaming potential. The was correlated by VES results showing materials with resistivity values ranging from (78.1 to 364.7 Ω.m, to depths ≥ 46 m). The streaming potential is attributed to groundwater flow, as against leachate as an electrical conductivity source, given the survey line's distance (about 300 m away) from the dumpsite.

3.11.4 Profile 6 (Control Centre)

This cross-section (Figure 15) correlates the VES log, 2-D ERT, SP profile, SP Contour and 3-D SP plot along profile 6 (Control Centre). The materials with low resistivity values ranging from

(32.6 to 71.2 Ω.m, to depths ≥ 12.4 m), stretching from (40 to 120 m), was interpreted as unconfined aquifer material. From the southern flank are materials with resistivity values ranging from (348 to 582 Ω.m, to depths ≥ 15.9 m), suggestive of fractured layer. Also inferred as fractured zone are objects with resistivity values ranging from (156 to 582 Ω.m, to depths ≥ 15.9 m) situated between (40 to 120 m). Comparatively, the resistivity values of (6.83 Ω.m) recorded near the dumpsite were lower than 32.8 Ω.m, recorded at the Control Centre. This established the presence of leachate contaminants near the dumpsite. The positive and negative variation of SP values ranging from (-90 to 120 mV) along the profile is attributed to groundwater streaming potential, while the materials with resistivity values ranging from (348 - 582 Ω.m, to depths ≥ 9.25 m),) located between (5 to 10 m), is diagnosed as fractured layer with potential for groundwater exploration.

3.12 Interpretation of Very Low Frequency Electromagnetic (VLF-EM) results

The results for the ten (10) VLF-EM Transverses 1 - 10 created adjacent the dumpsite indicating the fraser filtered, measured VLF and K-H pseudo cross-sections along transverses are shown in Figures 16 to 25:

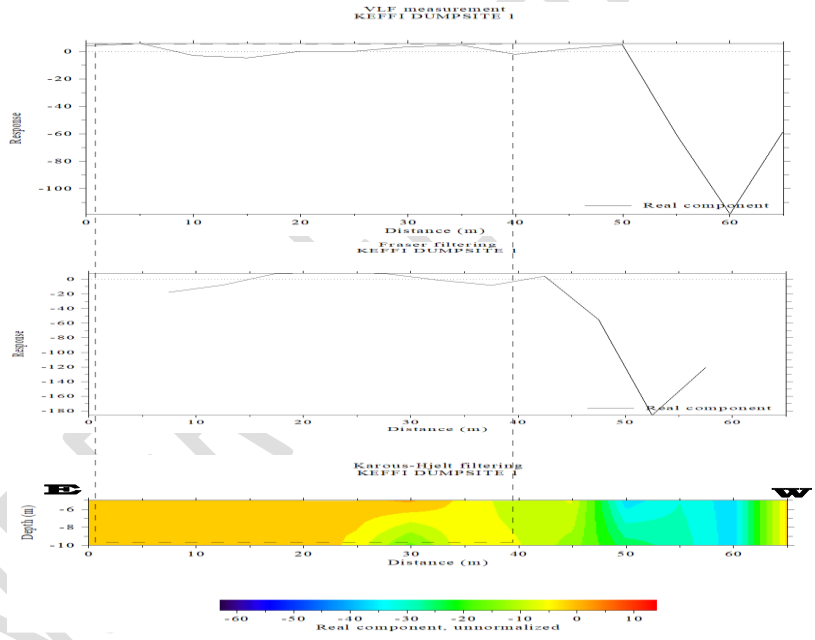

Figure 16: Cross-section of Fraser Filtered, measured VLF and K-H pseudo section along Transverse 1(Keffi)

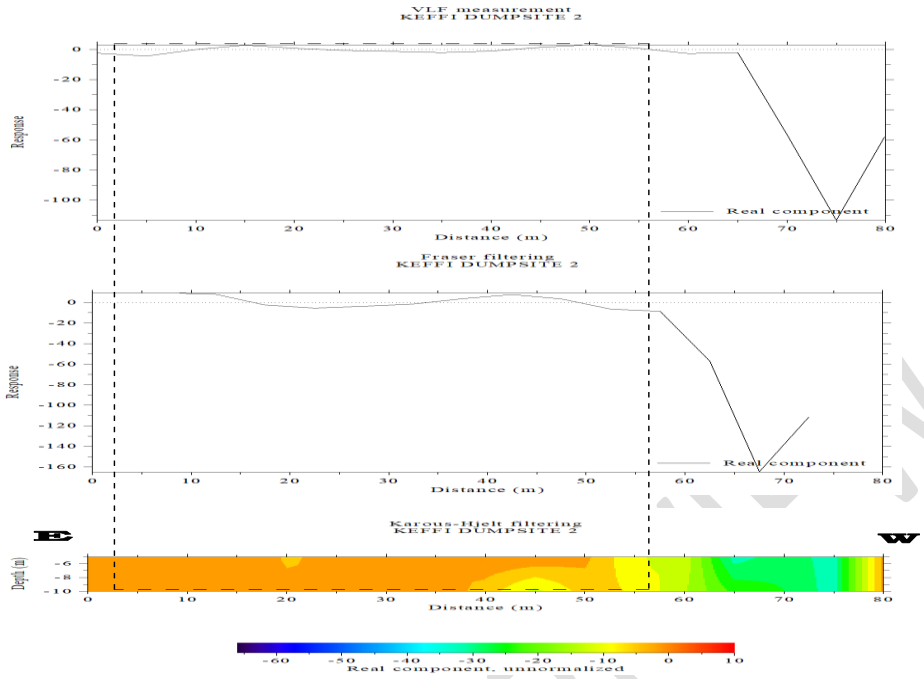

Figure 17: Cross-section of Fraser Filtered, measured VLF and K-H pseudo section along Transverse 2 (Keffi)

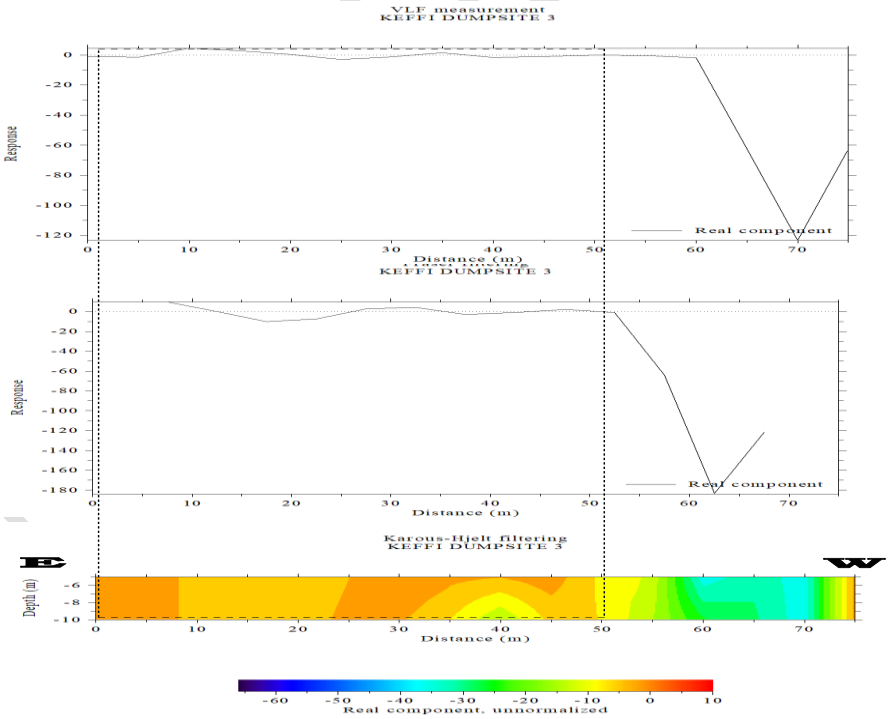

Figure 18: Cross-section of Fraser Filtered, measured VLF and K-H pseudo section along Transverse 3 (Keffi)

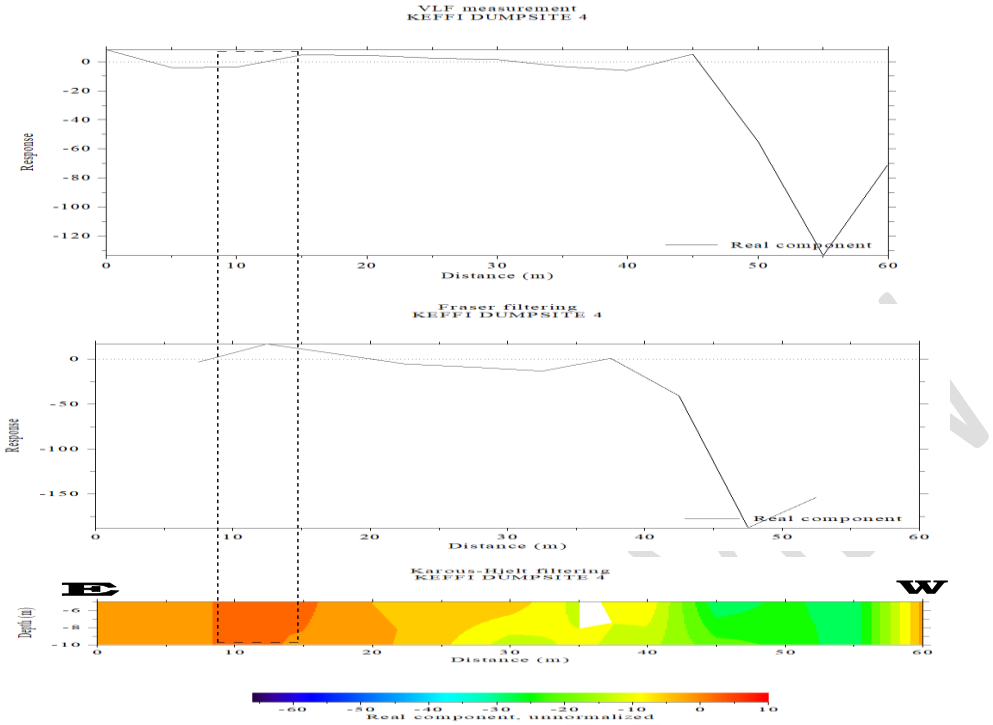

Figure 19: Cross-section of Fraser Filtered, measured VLF and K-H pseudo section along Transverse 4 (Keffi)

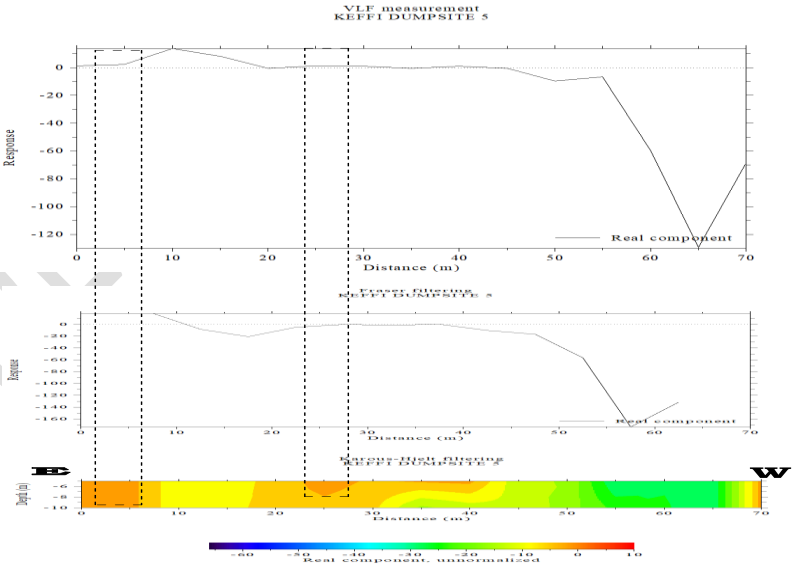

Figure 20: Cross-section of Fraser Filtered, measured VLF and K-H pseudo section along Transverse 5 (Keffi)

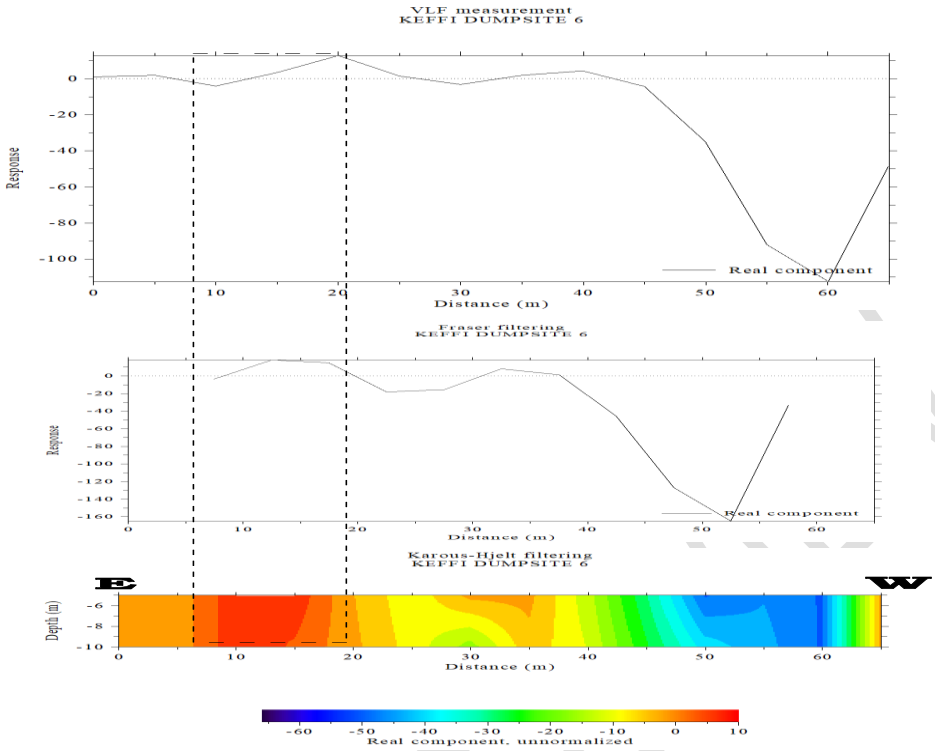

Figure 21: Cross-section of Fraser Filtered, measured VLF and K-H pseudo section along Transverse 6 (Keffi)

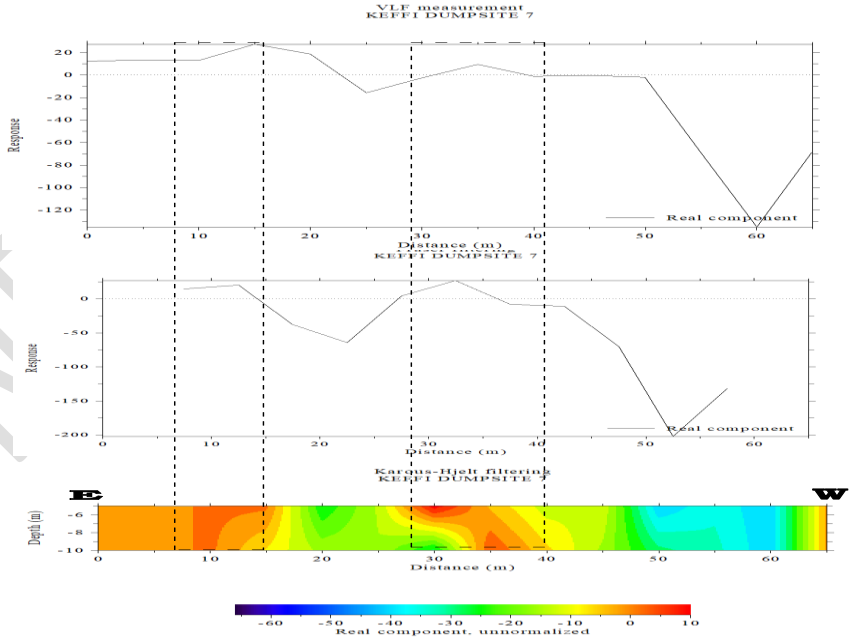

Figure 22: Cross-section of Fraser Filtered, measured VLF and K-H pseudo section along Transverse 7 (Keffi)

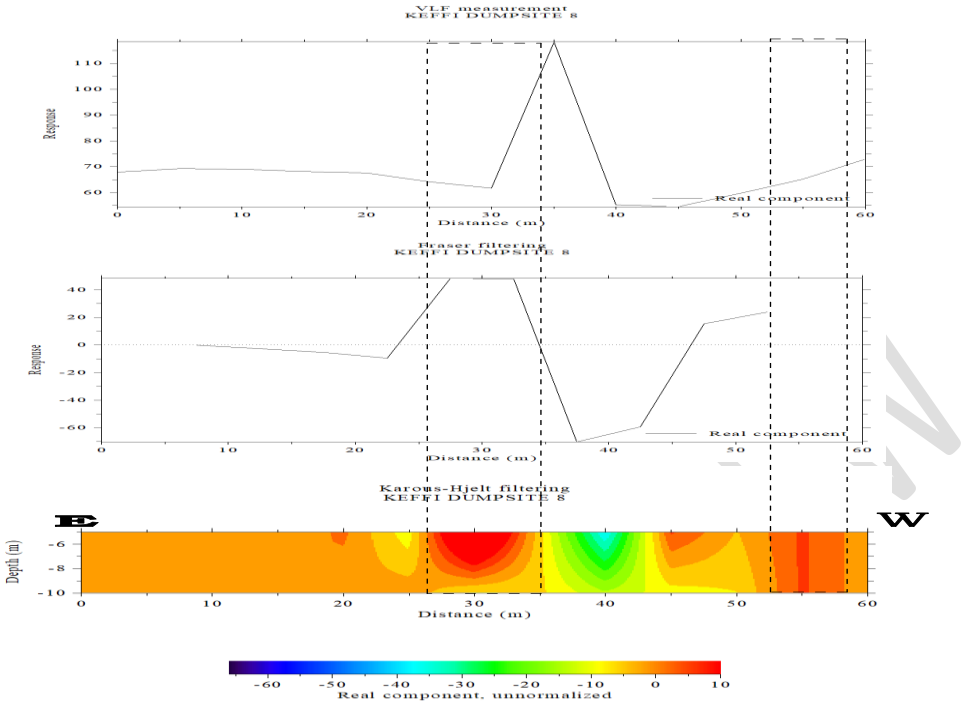

Figure 23: Cross-section of Fraser Filtered, measured VLF and K-H pseudo section along Transverse 8 (Keffi)

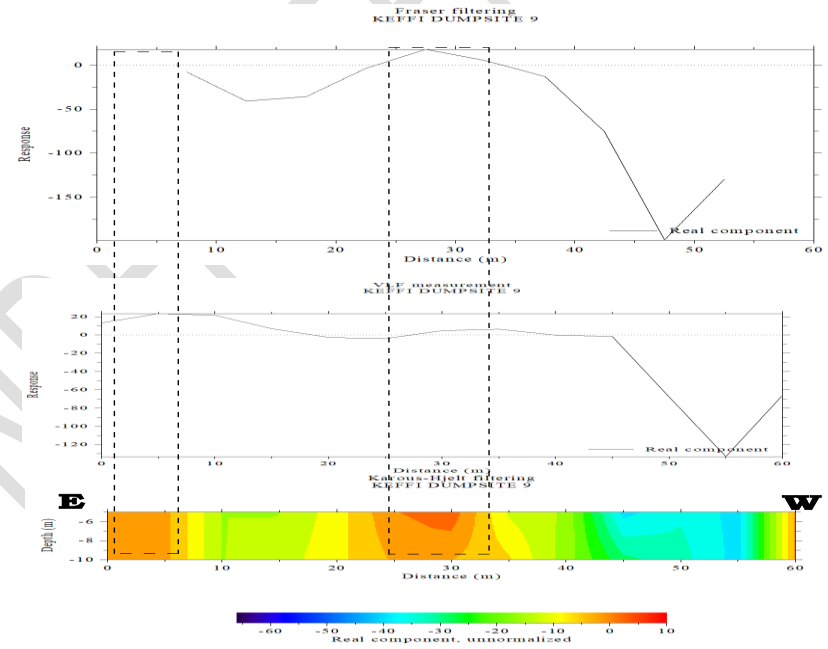

Figure 24: Cross-section of Fraser Filtered, measured VLF and K-H pseudo section along Transverse 9 (Keffi)

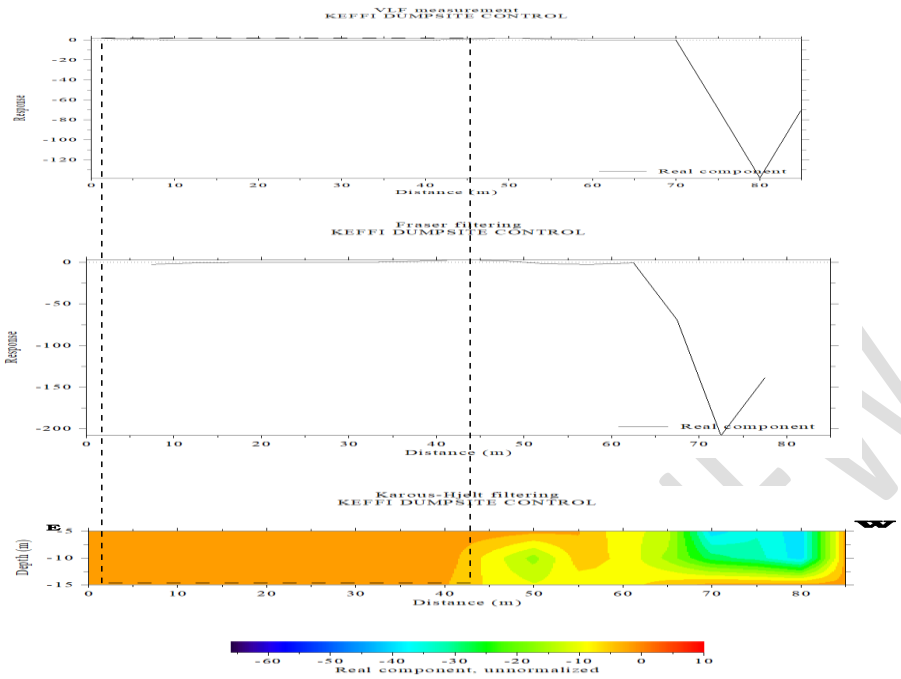

Figure 25: Cross-section of Fraser Filtered, measured VLF and K-H pseudo section along 10 (Keffi Control Centre)

3.13 Discussion

VLF-EM profiles 1 - 6 shows places of high positive current-density anomaly ranging from (-10 to 10 %) and covering (0 to 40 m) to depths of 10 m. This indicates lateral and vertical spread of leachate from the eastern to western part of the dumpsite into the subsurface. The areas with high negative anomaly ranging from (-20 to -60 %, to depths ≥ 14.5 m) covering (40 to 65 m) are interpreted as crystalline rocks with low conductivity. The strength of the positive anomaly, as reflected along profile 8, decreased as the profile distance from the dumpsite increased. The vicinity around 40 m – 65 m along profiles 1, 2, and 3 also show high positive anomaly that decreased in magnitude and size with distance from the Centre of the dumpsite. At profile 6, low positive current density indicates the absence of leachate at shallow subsurface. Places showing high positive current density are interpreted as soil and rocks infiltrated by leachate. The two VLF profiles located outside the dumpsite show lower current density (profiles 5, 6, 7, 8) than their corresponding profiles nearer the dumpsite (profiles 1, 2 and 3). This suggests that high current density is due to the presence of leachate. Along the Control Centre (Transverse 10), between (0 to 40 m) are materials with high positive current-density anomaly ranging from (0 to 5%, to depths ≥ 15 m), suggestive of groundwater saturated zones. In the western flank, are objects with high negative anomaly ranging from (-15 to -40 %, to depths ≥ 15 m) between (45 to 85 m), interpreted as low conductivity rocks.

3.14 Karu Dumpsite, FCT-Abuja

The summary of results for the three (3) VES points conducted within the Karu-Abuja dumpsite indicating the No. of layers, curve types, resistivity values (Ω.m), thicknesses (m), depth (m) and delineated lithological units are presented in Table 5:

Table 5: Vertical Electrical Sounding data for VES stations 1-3 (Karu-Abuja)

VES	No. of Layer (s)		Res	Thickness	Depth	Lithological Units
1	5	HA	294	0.6	0.6	Topsoil
			21.5	0.4	1	Weathered basement
			7.2	1	2	Weathered basement/leachate infiltrated
			221.7	1.4	3.4	Fractured basement
			57293.9			Fresh Basement
2	6	KHA	16.5	0.5	0.5	Topsoil (Lateritic)
			231.2	0.9	1.5	Weathered layer
			131.8	0.7	2.2	Weathered layer
			9.9	5.5	7.7	Weathered basement/leachate infiltrated
			346.3	35.2	43	Fractured basement
			478.8			Fractured basement
3	5	QA CC	74.4	0.7	0.7	Topsoil (Lateritic)
			21.4	2.2	2.9	Weathered basement
			11.4	5.8	8.7	Weathered basement/leachate infiltrated
			419.8	12.1	20.8	Fractured basement
			1932.6			Fresh Basement

3.15 Estimated Aquifer Parameters of the surveyed area (Karu-Abuja)

The primary aquifer parameters (resistivity and thickness) are determined from Table 8 and used to estimate the geo-hydraulic parameters. The summary of the Daz-Zarrouk parameters estimated for the weathered aquifers within Karu Dumpsite showing the VES points, resistivity values ρ (Ω.m), Aquifer thicknesses h (m), Electrical conductivity σ (Ω.m^{-1}), Longitudinal Conductance S (mhos), Transverse Resistance T_R (Ω.m^{-2}), Hydraulic conductivity K (m/day), Transmissivity T (m^2/day), quantity of water and porosity ϕ (%) are presented in Tables 6 and 7:

Table 6: The summary of Dar Zarrouk parameters and electrical conductivity K (m/day) estimated for the weathered aquifers in the study area (Karu-Abuja)

VE S	ρ (Ω.m)	Thickness (h)	σ = 1/ ρ	S = σh	R = hρ	K (m/day)

1	221.7	1.4	0.0045	0.006	310.38	2.51
2	346.3	35.2	0.0029	0.10	12189.7	1.65
3	419.8	12.1	0.0024	0.03	5079.6	1.38

Table 7: The summary of aquifer transmissivity (T), quantity of water Q and porosity ϕ (%) estimated for the weathered aquifers in the study area (Karu-Abuja)

VES	Tr = kh	Quantity (kσ)	Porosity (ϕ) (%)
1	3.51	0.0113	29.63
2	58.2	0.0048	27.76
3	16.7	0.003	26.95

3.16 Results of computer modeled curve for three (3) VES points (Karu-Abuja)

The results of the computer modeled curves for the three (3) VES points conducted within the study area are shown in Figures 26 to 28:

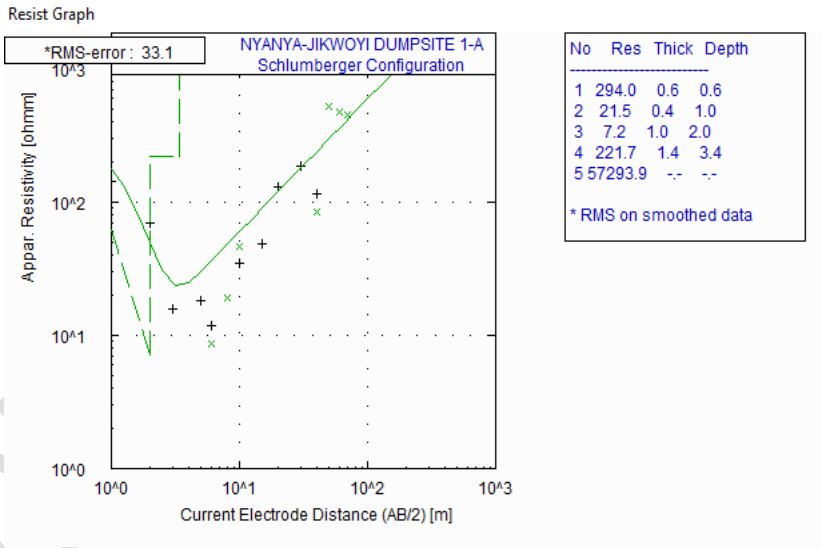

Figure 26: Results of computer modeled curve for VES 1

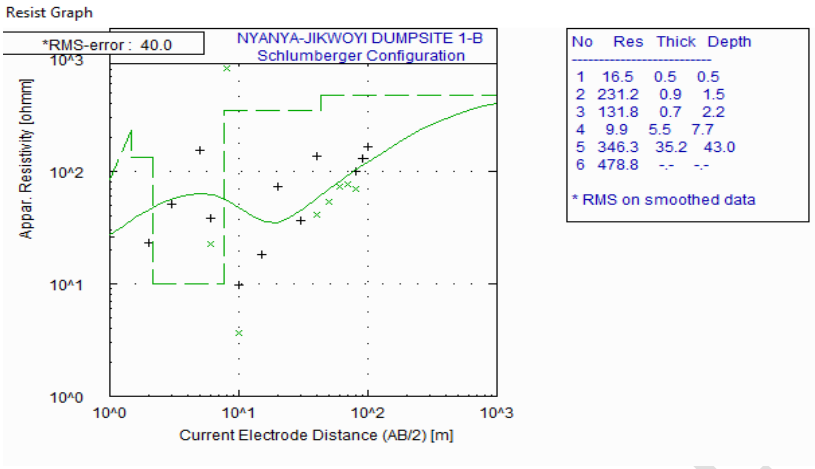

Figure 27: Results of computer modeled curve for VES 2

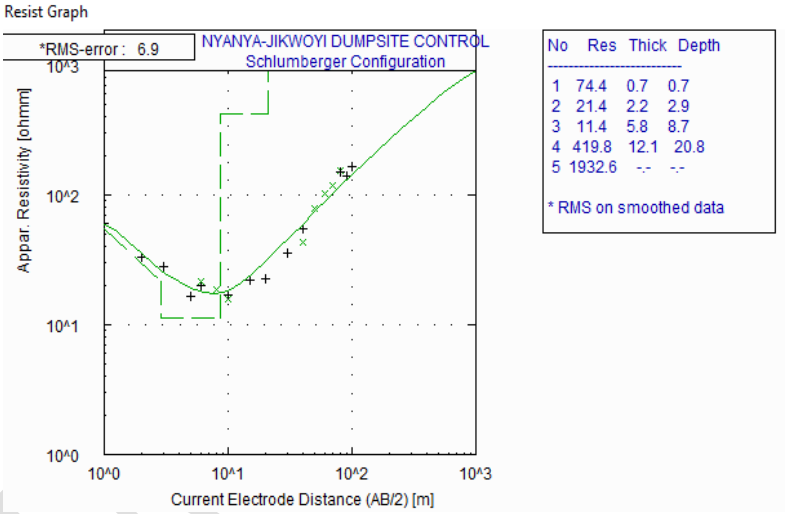

Figure 28: Results of computer modeled curve for Control Centre

3.16.1 Correlation of Borehole log with VES (Karu-Abuja)

The correlation of borehole lithological logs BH (after Sunkari *et al.* 2021) with resistivity sounding (VES) results for VES 1-3 in the study area are shown in Figures 29:

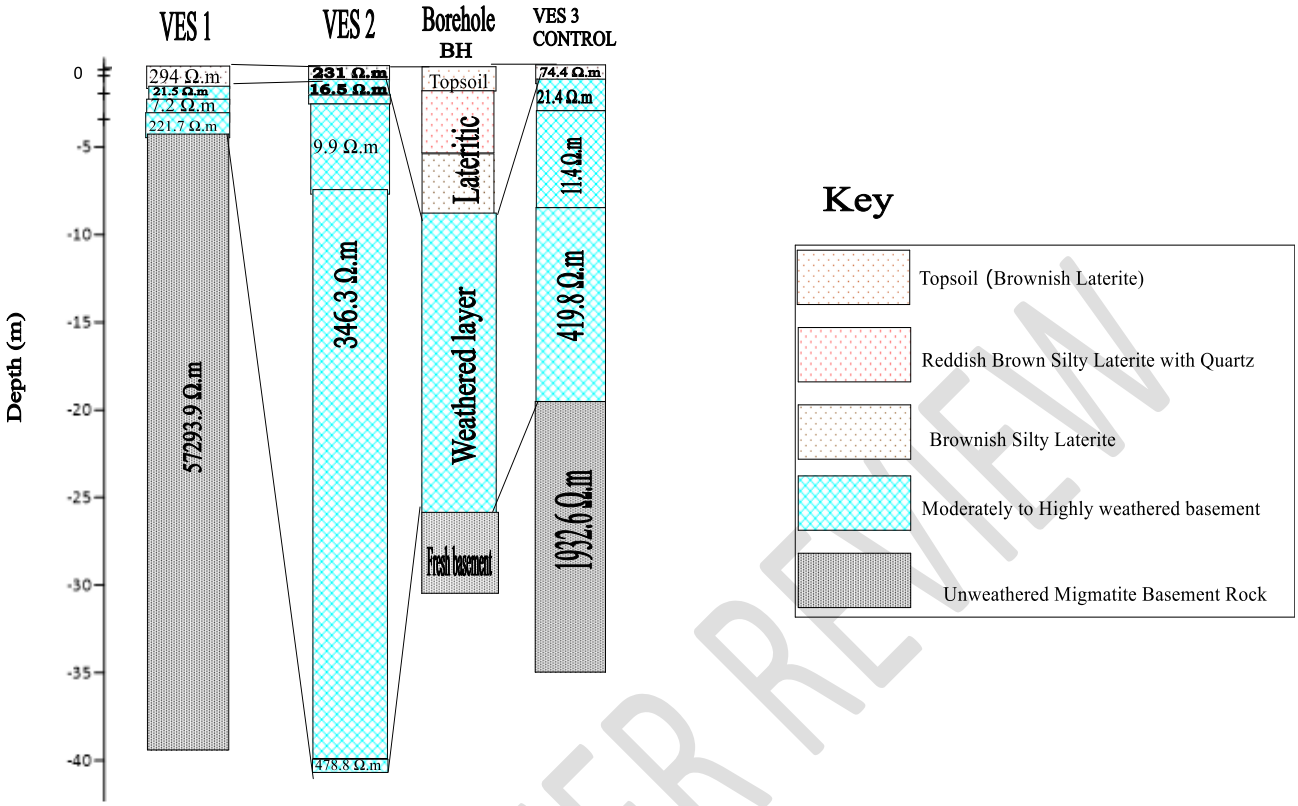

Figure 29: Correlation of resistivity sounding (VES) results with borehole lithological logs in the study area (Karu-Abuja)

3.17 Discussion

The measured apparent resistivity curves and results of the 1-D inversion are displayed in the corresponding resistivity-depth profiles (Figures 26 to 28). The VES data revealed five to six discrete geo-electric layers, such as the Topsoil consisting of lateritic soil, second layer interpreted as clayey sand, third layer inferred as weathered layer, fourth layer interpreted as fractured, the fifth and sixth layers, interpreted as fresh bedrock. The Curve Types identified from the model include: HA (33.3%), KHA (33.3%), and type QA (33.3%), identified at the Control Centre.

Table 5 shows the resistivity values, thicknesses, depth and lithological units for each of the electro-stratigraphic layers within the maximum current electrode separation along the transverses. The study area is characterised by heterogeneous lithology with resistivity values varying from low to high. The primary aquifer parameters (resistivity and thickness) are determined from Table 5 and used to estimate the geo-hydraulic parameters (Table 6 and 7). The geo-electric sections revealed five to six discrete geo-electric layers, consisting of Topsoil (lateritic), weathered layer (clayey sand), fractured and fresh bedrock.

3.18 The Topsoil

Resistivity values for Top soil layers and their corresponding thicknesses varies from VES 1 (294.0 to 21.5 Ω.m), (0.6 to 0.4 m), VES 2 (16.5 to 231.2 Ω.m), (0.5 to 0.9 m), VES 3 (74.4 to 21.4 Ω.m),

(0.7 to 2.2 m). This is suggestive of three zones: the belt of the soil water at the top, the intermediate vadose zone, and the capillary fringe at the bottom which acts as the passage for the flow of surface water to the fractured layer known as the zone of aeration.

3.19 The Second layer

Resistivity values for second layers and their corresponding thicknesses varies from VES 1 (21.5 to 7.2 Ω.m), (0.4 to 1.0 m), VES 2 (231.2 to 131.8 Ω.m), (0.9 to 0.7 m), VES 3 (21.4 to 11.4 Ω.m), (2.2 to 5.8 m). This layer is mostly composed of weathered to fresh basement, clay, and consolidated sandstone. The varying levels of compaction in the sandy clay material may account for the contrasting resistivity values in this layer. This layer is characterized by priority targets for groundwater exploration.

3.20 The third layer

Resistivity values for the third layers and their corresponding thicknesses varies from VES 1 (7.2 to 221.7 Ω.m), (1.0 to 1.4 m), VES 2 (131.8 to 9.9 Ω.m), (0.7 to 0.7 m), VES 3 (11.4 to 419.8 Ω.m), (5.8 to 12.1 m). This layer is mostly composed of fractured bedrock and consolidated sandstones.

3.21 The fourth layer

Resistivity values for the fourth layers and their corresponding thicknesses varies from VES 1 (221.7 to 57,293.9 Ω.m), (1.4 m to infinity), VES 2 (9.9 to 346.3 Ω.m), (5.5 to 35.2 m), VES 3 (419.8 to 1,932.6 Ω.m), (12.1 m to infinity). This layer is mostly composed of fractured to fresh basement.

3.21.1 The fifth/sixth layer

Resistivity values for fifth layer and their corresponding thicknesses varies from VES 1 (57, 293.9 Ω.m to infinity), (1.4 m to infinity), VES 2 (346.3 to 478.8 Ω.m), (35.2 m to infinity), VES 3 (1,932.6 Ω.m to infinity). This layer is mostly composed of fresh basement.

3.22 The conductive layers

The study has shown that leachate has spread along transverse 1 and 2 and occurs at a maximum depth of 5.5 m at an average depth of 3.25 m. This was correlated by 2-D ERT real inverse models.

3.23 Estimated Aquifer Protective Capacity (APC) for the study area (Karu-Abuja)

The calculated Longitudinal Conductance S (Table 8) revealed that the aquifer protective capacity of the study area is rated as poor to weak; with two VES points VES 1 (0.0063 S) and VES 3 (0.002 S), representing 66.6% of the sounding points, indicating poor protective capacity; while VES point VES 2 (0.1 S) representing 33.3% of the soundings, shows weak protective capacity.

3.24 Delineation of aquifer systems

A borehole log (after Sunkari *et al.* 2021) was used to correlate with VES points along the profiles and used to infer the lithologic sections derived from the interpretations of VES profiles (1 to 3) around the dumpsite and the Control Centre with a view to delineating the aquifer systems in the area.

3.25 Results of the Self-Potential (SP) survey conducted within the study area (Karu-Abuja)

The results of the four (4) Self-Potential (SP) profiles conducted in the study area are shown in Table 8:

Table 8: Summerised results from Self-Potential (SP) survey in the study area

Distance X (m)		SP (mV) 1	SP (mV) 2	SP (mV) 3	SP (mV) 4 Control
0		160.1	-206.9	-22.44	88.1
5		-338.8	-215.1	30.22	-74.4
10		-268.8	-196.8	-424.2	-56.8
15		-304.4	-191.7	20.59	-81.4
20		-326.7	-185.6	23.05	-62.7
25		-328.7	-173.5	23.36	100.5
30		-333.5	-170.4	40.16	88.9
35		328.7	-164.3	112.7	69.1
40		338.9	-142.4	1.762	56.2
45		338.9	-107.5	25.82	-87.5
50		350.0	-84.43	25.61	-174.1
55		-341.1	-98.17	65.17	-172.2
60		-344.9	-3.432	17.72	-152.6
65		-363.2	-6.64	24.08	-179.6
70		-353.1	-22.33	27.76	-131.1
75		-349.0	9.078	-3.072	-56.8
80		347.0	-5.70	-40.78	-95.7
85		337.8	42.62	-17.62	-44.5
90		337.8	35.96	-2.910	-62.3
95		-339.9	46.11	-	-

3.26 CORRELATION ANALYSIS

The following cross-sections correlates the Self Potential (mV) profiles, SP contours and 3-D SP plots, the VES transverses and 2-D ERT geo-electric sections along the survey lines (Figures 30 – 33):

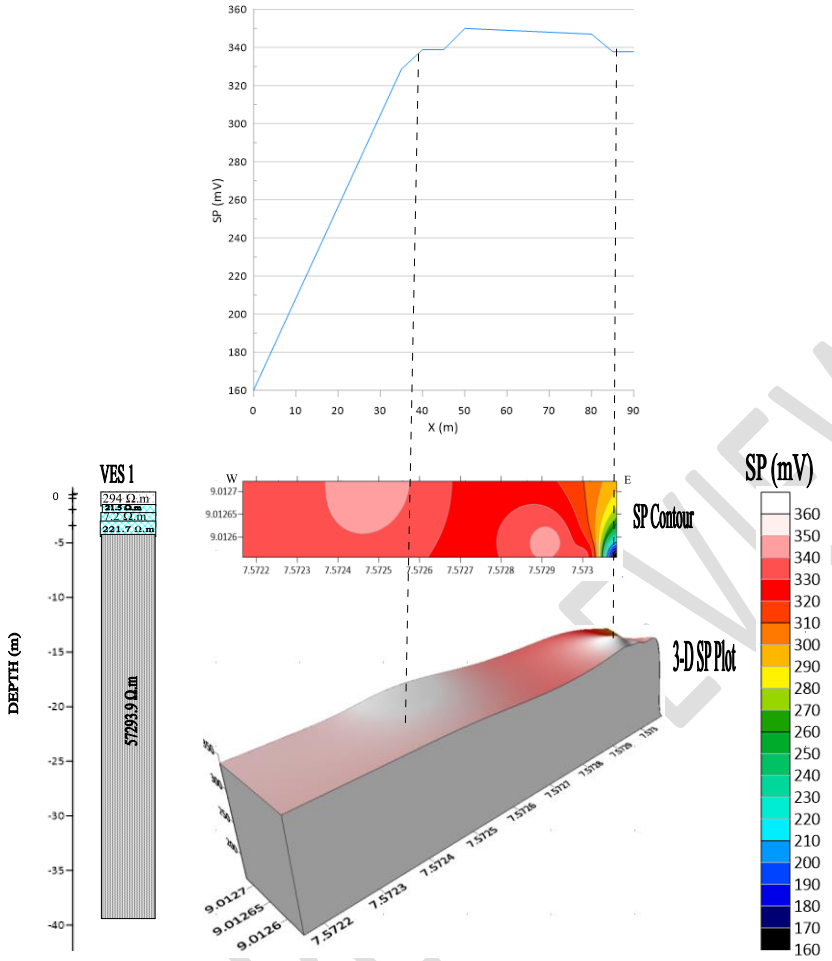

Figure 30: Cross-section correlating the SP profile, SP contours and 3-D SP plot and VES log along Profile 1 (Karu-Abuja)

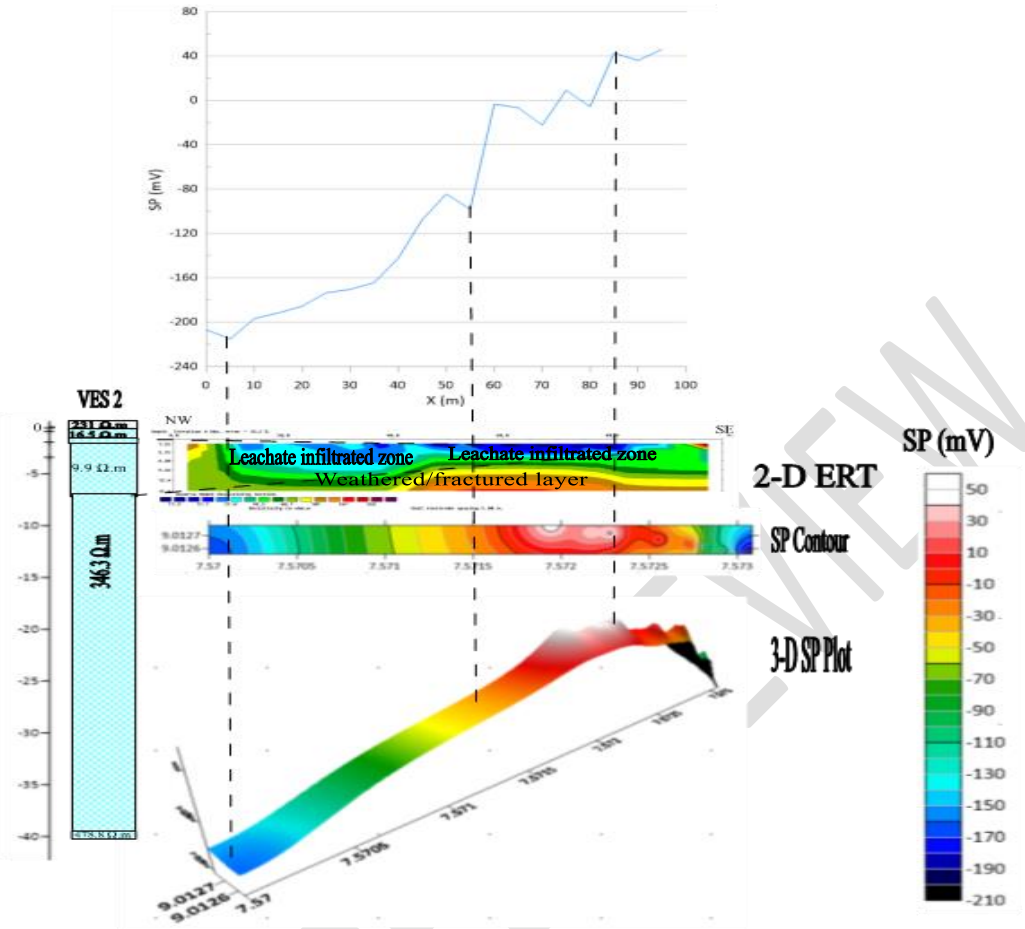

Figure 31: Cross-section correlating the SP profile, SP contours and 3-D SP plot and VES log along Profile 2 (Karu-Abuja)

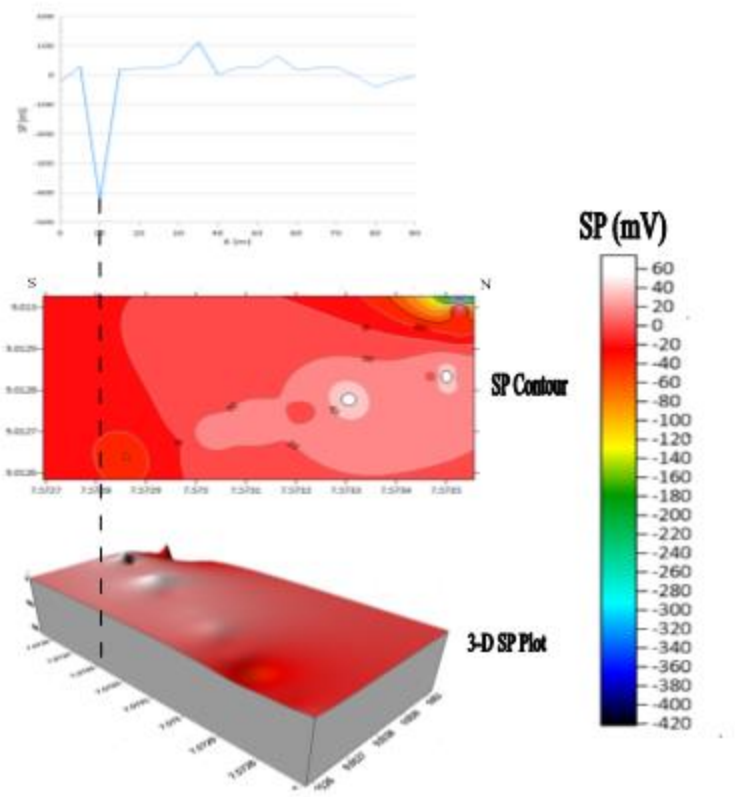

Figure 32: Cross-section correlating the SP profile, SP contours and 3-D SP plot and VES log along Profile 3 (Karu-Abuja)

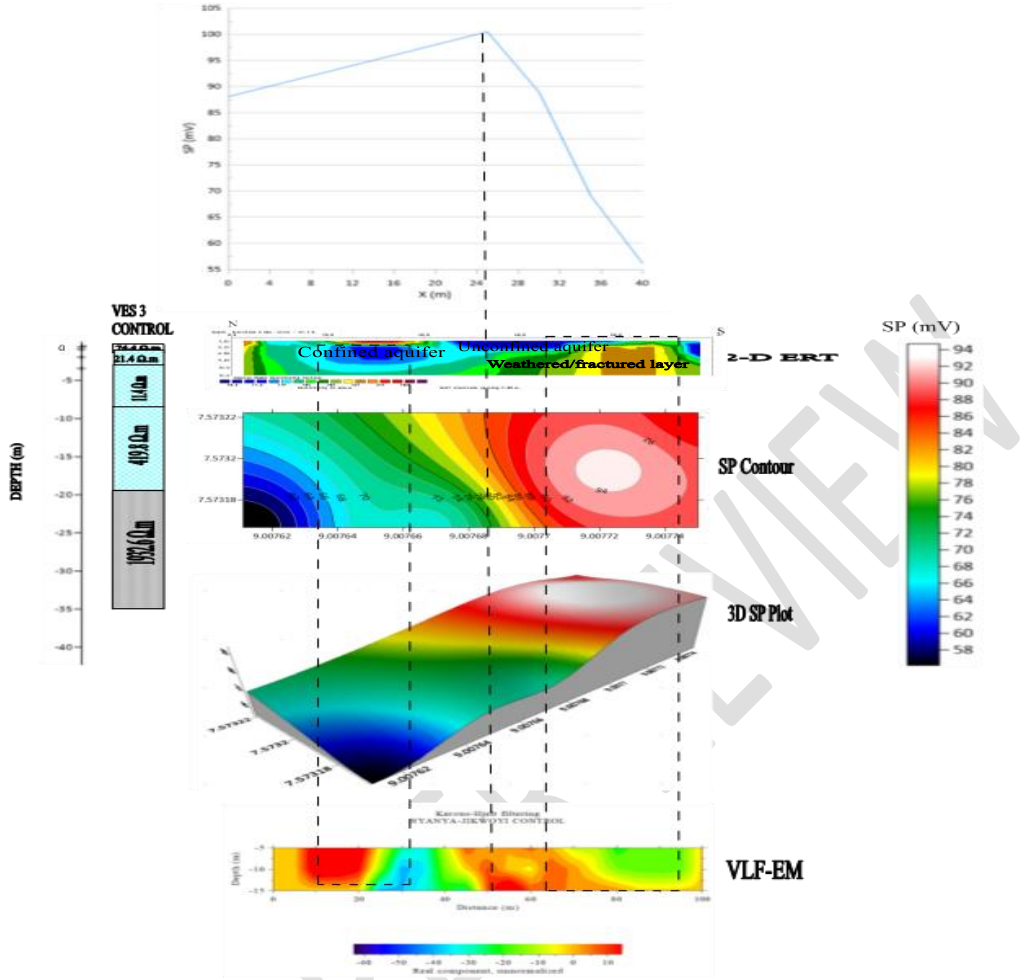

Figure 33: Cross-section correlating the SP profile, SP contours and 3-D SP plot and VES log along Profile 4 (Karu-Abuja Centre Centre)

3.27 DISCUSSION

3.28 Profile 1

This cross-section (Figure 30) correlates the SP profiles, SP contours, 3-D SP and VES Log. The SP profile shows positive SP anomalies ranging from (160 to 360 mV) between (0 – 90 m) diagnosed as streaming potentials attributed to an adjourning stream and leachate flow in the E–W direction. This was correlated by materials with low resistivity value of (7.2 Ω.m, depths ≥ 2.0 m) from the VES log interpreted as leachate plume.

3.29 Profile 2

This cross-section (Figure 31) correlates the SP profile, 2-D ERT, SP contours and 3-D SP plot for profile 2. The 2-D ERT geo-electric section identified three layers. The Topsoil (consisting of laterite soil and leachate infiltrated zones); the weathered and the fractured basement. The materials with low resistivity values ranging from (11.3 to 15.9 Ω.m, to depths ≥ 6.63 m) spread between (0 – 100 m) suggests leachate infiltrated zone flowing in the NW - SE direction. From the

NW flank, is a material with resistivity value ranging from (27.8 to 66.8 Ω.m, to depths ≥ 12.4 m) situated between (0 to 40 m) interpreted as weathered layer. Between (50 to 100 m) are materials with resistivity values ranging from (187 to 262 Ω.m), interpreted as deep seated fracture acting as water conduits to the vadose zone. The proximity of a protruding material in the southeastern axis, interpreted as leachate plume, suggests that groundwater resources in the area must have been contaminated by leachate. The dominant negative SP anomalies ranging from (-210 to -1 mV) along the survey line, which increased exponentially at the central point, were similarly correlated as leachate accumulation. The positive SP anomalies beyond (60 m to 100 m) were diagnosed as bioelectric materials emanating from decomposing corpses from a cemetery adjacent the study area. The 2-D ERT and SP results were correlated by the VES geo-electric section along the survey line which revealed the presence of low resistivity materials ranging from (9.9 to 16.5 Ω.m, to depths ≥ 7.7 m) suggestive of leachate infiltrated zone.

3.30 Profile 3

This cross-section (Figure 32) compares the SP profile, SP contour and 3-D SP plots for profile 3. The dominant negative SP anomaly ranging from (-420 to -20 mV) which peaked between (0 – 10 m) is attributed to redox reaction influenced by deep seated leachate accumulation. Further away from the dumpsite, between (20 to 90 m) was rebound with a positive SP anomaly ranging from (0 to 60 mV). This was interpreted as streaming potentials.

3.30.1 Profile 4 (Control Centre)

This cross-section (Figure 33) correlates the SP profile, the 2-D ERT, SP contours, 3-D SP plot and VES log for the Control Centre. The low resistivity materials from the northern flank, ranging from (50.4 to 77.6 Ω.m, to depths ≥ 12.4 m) situated beneath a suspected clay seal between (20 to 40 m) is interpreted as a confined aquifer with groundwater potential. On the southern flank is a material with resistivity values ranging from (50.5 to 60 Ω.m, to depths ≥ 6.3 m) situated between (40 to 80 m), diagnosed as an unconfined aquifer. Between (0 to 50 m) are materials with resistivity values ranging from (119 to 283 Ω.m, to depths ≥ 15.9 m). This is interpreted as a weathered layer. Materials with resistivity values ranging from (438 to 673 Ω.m, to depths ≥15.9 m) located on the northern flank; between (60 to 100 m), is suggestive of a fractured basement. This was correlated by VES log showing materials with resistivity values ranging from (11.4 to 419.8 Ω.m, to depths ≥ 8.7 m) along the transverse. The dominant positive SP anomalies ranging from (58 to 94 mV) along the survey line, suggests the presence of geochemical reactions attributed to groundwater flow in the S-N direction. The VLF-EM similarly shows material with positive current-density ranging from (5 to 10 %) situated along (10 to 20 m and 40 to 70 m, to depths ≥ 15 m) along the survey line. This is suggestive of weathered/fractured materials hosting groundwater resources.

3.31 Interpretation of Very Low Frequency Electromagnetic (VLF-EM) results

The results for the six (6) VLF-EM Transverses 1 - 6 created adjacent the dumpsite indicating the fraser filtered, measured VLF and K-H pseudo cross-sections along transverses (Figures 34 to 39):

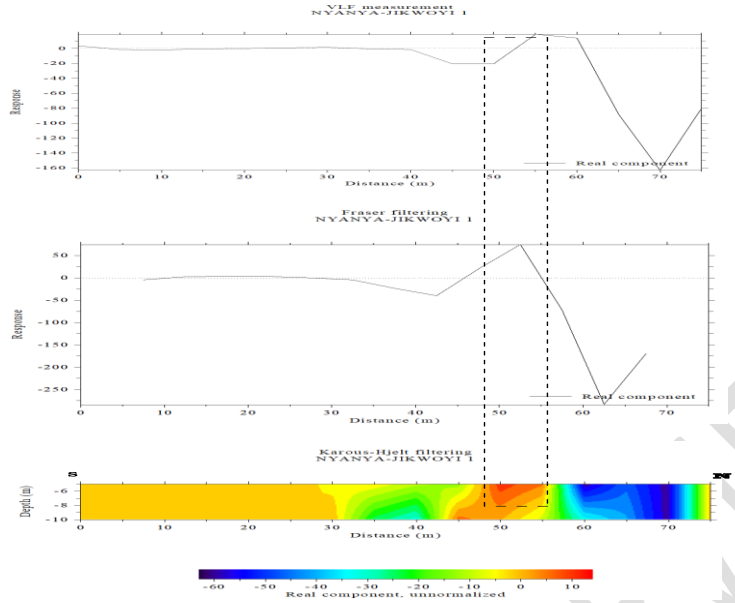

Figure 34: Cross-section of Fraser Filtered, measured VLF and K-H pseudo section along Transverse 1 (Karu-Abuja)

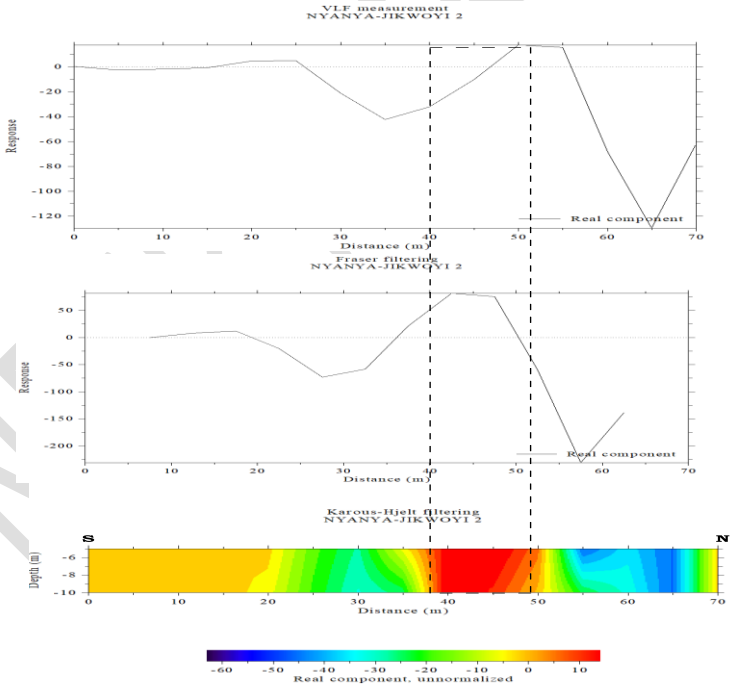

Figure 35: Cross-section of Fraser Filtered, measured VLF and K-H pseudo section along Transverse 2(Karu-Abuja)

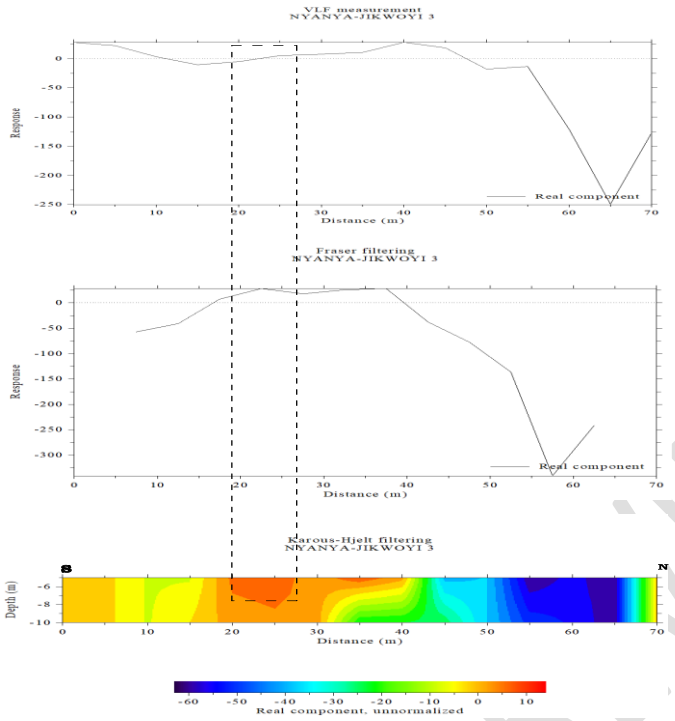

Figure 36: Cross-section of Fraser Filtered, measured VLF and K-H pseudo section along Transverse 3 (Karu-Abuja)

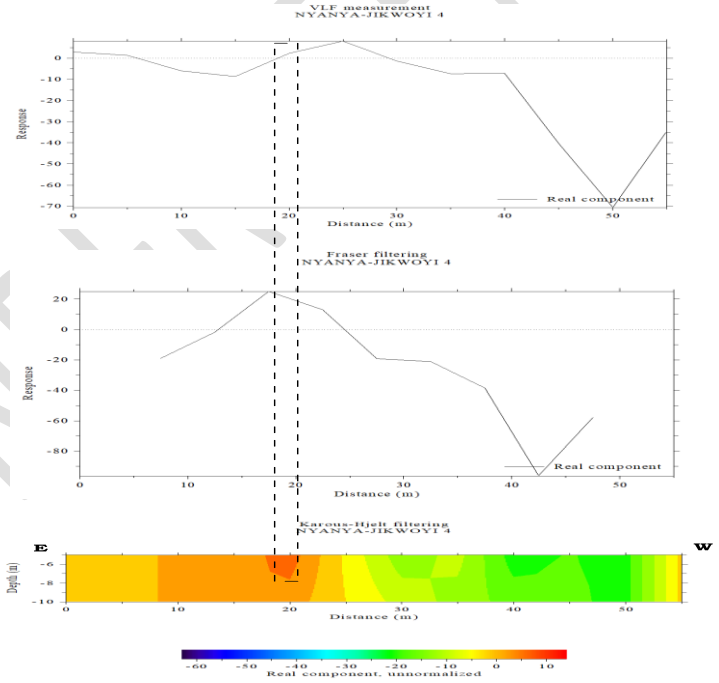

Figure 37: Cross-section of Fraser Filtered, measured VLF and K-H pseudo section along Transverse 4(Karu-Abuja)

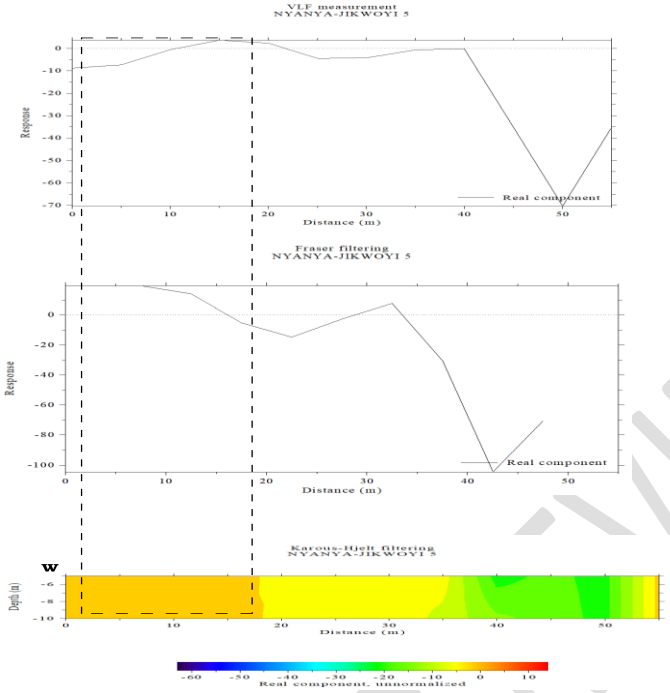

Figure 38: Cross-section of Fraser Filtered, measured VLF and K-H pseudo section along Transverse 5 (Karu-Abuja)

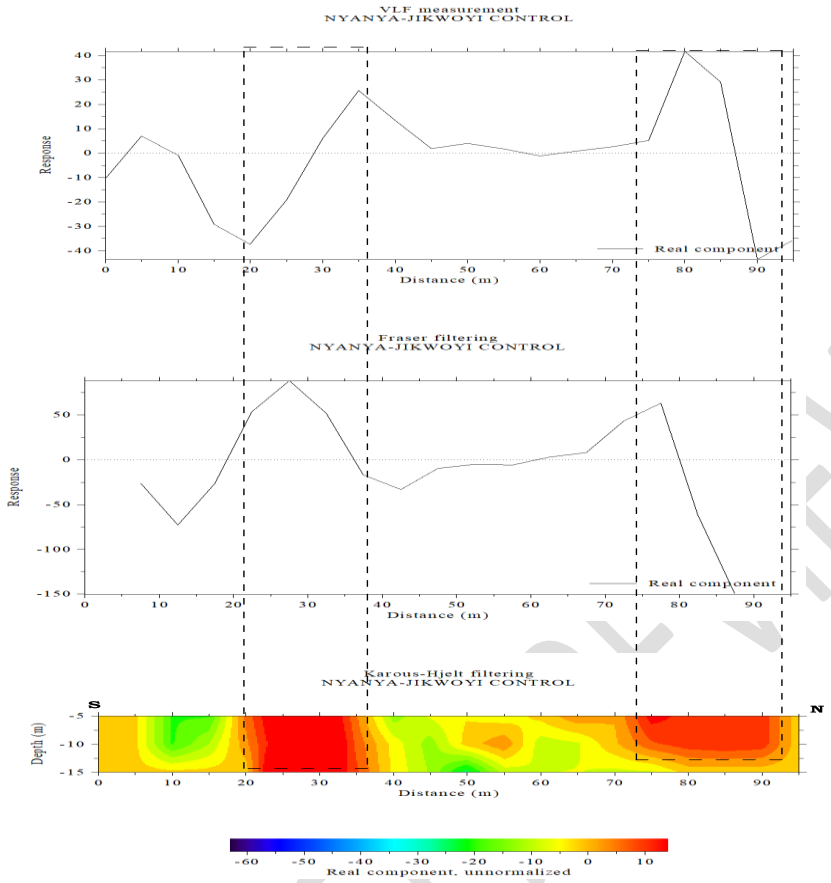

Figure 39: Cross-section of Fraser Filtered, measured VLF and K-H pseudo section along Transverse 6 (Control Centre)

3.31.1 Discussion

3.31.2 Transverse 1

From the starting point of (Figure 34) along the survey line, between (0 to 30 m) are yellowish materials with current density ranging from (-5 to 5 %, to depths ≥ 15 m) suggestive of conductive materials flowing in the S – N direction. Between (40 to 51 m) along the profile are reddish prominent materials with high positive anomaly ranging from (5 to 10%, to depths ≥ 10 m). This is suggestive of leachate generated electrical conducting paths. Between (30 to 42 m) are greenish materials with negative anomaly ranging from (-10 to -25 %) suggestive of rock intrusions. Between (60 to 80 m) are bluish materials with negative current density (-10 to -60 %) suggestive of fractured bedrock.

3.31.3 Transverse 2

From the starting point (0 to 20 m) along the survey line (Figure 35) are yellowish materials with current density ranging from (-5 to 5 %) suggestive of conductive materials flowing in the S – N direction. However, between (40 to 51 m) along the profile are reddish materials with prominent high positive anomaly ranging from (5 to 10%) along the survey line. This is suggestive of lateral and vertical spread of leachate into the subsurface. Between (20 to 37 m) are greenish materials

with negative anomalies ranging from (-10 to -25 %) suggestive of intercalations of clay and sandstones. Between (51 to 70 m) are bluish and greenish materials with negative current-densities ranging from (-10 to -60 %) suggestive of fractured bedrock.

3.31.4 Transverse 3

From the starting point (0 to 20 m) along the survey line (Figure 36) are yellowish and greenish materials with current density ranging from (-20 to 1 %) suggestive of conductive materials flowing in the S – N direction. However, between (20 to 30 m) along the profile are materials with prominent high positive anomaly ranging from (5 to 11 %) along the survey line. This is suggestive of leachate generated electrical conducting paths. Between (30 to 50 m) are greenish materials with negative anomalies ranging from (-20 to -30 %) suggestive of hardpan. At distances between (50 to 70 m) are deep bluish and greenish materials with negative current densities ranging from (-10 to -65 %) suggestive of fractured bedrock.

3.31.5 Transverse 4

The material (Figure 37) with high positive anomaly ranging from (5 to 10 %) between (10 to 25 m) is suggestive of lateral and vertical spread of leachate flowing in the E – W direction. Between (0 to 10 m) is yellowish material with high negative and positive current densities anomaly ranging from (-5 to -5 %, to depths ≥ 10 m) suggestive of lateritic soil. Between (25 to 60 m), are intercalations of greenish and lemon materials suggestive of lineament structures.

3.31.6 Transverse 5

Starting from (0 to 10 m) (Figure 38) are yellowish materials with negative and positive current density anomaly ranging from (-5 to 5 %) suggestive of leachate infiltrated zones flowing in the W – E direction. Between (20 to 35 m) are yellowish materials suggestive of lineament structures. Between (35 to 60 m) are patches of greenish and yellowish materials with current density ranging from (-20 to -5 %) suggestive of mineralized pegmatite which outcrops the study area.

3.31.7 Transverse 6 (Control Centre)

Transverse 6 (Figure 39) is the Control Centre situated approximately 500 m away from the dumpsite. The results revealed that materials with prominent positive current-density ranging from (5 to 10 %) situated along (10 to 20 m and 40 to 70 m, to depths ≥ 15 m) is suggestive of weathered/fractured materials hosting groundwater resources. Between (20 to 40 m) and (80 to 100 m) are blue, green and yellow patches suggestive of mineralised intrusions.

4. Summary and Conclusion

The study used integrated geophysical methods to assess aquifer vulnerability in Karu-Abuja and Keffi, comparing the susceptibility of aquifer systems to leachate contamination. This involved the establishment of nine VES points using the Schlumberger array, four 2-D ERT profiles using the Wenner configurations, ten SP profiles, and sixteen VLF transverses near the dumpsites and the control areas. The Ohmega (Allied Geophysics) resistivity meter and Gem portable receiver systems were used to acquire the data, while interpretation of data employed tools such as WINRESIST, RES2DINV, GRAPHER, SURFER and KHFFILT. These methods identified groundwater saturation zones and contamination pathways, including fractures and faults. The

resistivity values of the topsoil which ranges from (47.1 to 224.2 Ω.m) and (16.5 to 294.0 Ω.m) extending to depths ≥ 2.1 m and 0.5 m in Karu-Abuja and Keffi respectively, suggests that the overburden of study areas are composed of low-permeable unconsolidated clay, sandy, and gravel materials. The estimated Aquifer Protective Capacity (APC) from the VES resistivity data, indicated poor to good rating for Keffi, and poor to weak for Karu-Abuja, which were validated by the borehole logs. Results revealed that Keffi has appreciably thicker overburden than the Karu-Abuja study areas and thus, better aquifer protective layers. Comparatively, the findings revealed that the Keffi study areas possess better impervious clay seals to protect groundwater resources against leachate infiltration than the Karu-Abuja. Regular Environmental Impact Assessments (EIAs) and the installation of geo-synthetic clay liners at the base of the dumpsites to safeguard groundwater resources from leachate infiltration are therefore recommended.

REFERENCES

Abdel-Shafy, H. I., Ibrahim, A. M., Al-Sulaiman, A. M., & Okasha, R. A. (2024). Landfill leachate: Sources, nature, organic composition, and treatment: An environmental overview. *Ain Shams Engineering Journal*, *15*(1), 102293.

Ajibade, A. C., and Fitches, W. R. (1988). The Nigerian precambrian and the Pan-African orogeny. Precambrian geology of Nigeria, 1, 45-53.

Anudu, G.K., Obrike, S.E. and Ofoegbu, C.O. 2021 Groundwater Investigation Across the Crystalline Basement Rocks in Rogo Area, Kano State Northern Nigeria, Using Resistivity Methods (Keffi Borehole log)

Arthur, J. C. (2024). Water Quality and Health Risk Assessment of Ground Water from Dump Site around Uguwaji Waste Dumpsite, Enugu Metropolis.

Bashir, M. Z. (2018). Geology of The Area Around Kurafe Hausawa, Part of Keffi Sheet 208 nw. 61.

Chinyem, F. I., & Ovwamuedo, G. (2024). Evaluation of aquifer characteristics and groundwater protective capacity in Abavo, Nigeria. International Journal of Geosciences, 15(11), 841-860.DOI: 10.4236/ijg.2024.1511046

Chinyem, F.I. Determination of aquifer hydraulic parameters and groundwater protective capacity in parts of Nsukwa clan, Nigeria. *Environ Monit Assess* 196, 243 (2024). DOI: https://doi.org/10.1007/s10661-024-12411-w

Dada, S. S. (2006). Proterozoic evolution of Nigeria. The basement complex of Nigeria and its mineral resources (A Tribute to Prof. MAO Rahaman). Akin Jinad and Co. Ibadan, 29-44.

Ejepu, J. S., Jimoh, M. O., Abdullahi, S., Abdulfatai, I. A., Musa, S. T., & George, N. J. (2024). Geoelectric analysis for groundwater potential assessment and aquifer protection in a part of Shango, North-Central Nigeria. *Discover Water*, *4*(1), 33.

Huang, P., Hou, M., Sun, T., Xu, H., Ma, C., & Zhou, A. (2024). Sustainable groundwater management in coastal cities: Insights from groundwater potential and vulnerability using ensemble learning and knowledge-driven models. *Journal of Cleaner Production*, *442*, 141152.

Ishola, S. A. (2024). Aquifer Characteristics and Groundwater Reservoir Protective Capacity Rating in Obafemi-Owode LGA, Ogun State South-West, Nigeria.

Koliyabandara, P. A., Preethika, D. D. P., Cooray, A. T., Liyanage, S. S., Siriwardana, C., & Vithanage, M. (2024). The Environmental Pressure by Open Dumpsites and Way Forward. In *Technical Landfills and Waste Management: Volume 1: Landfill Impacts, Characterization and Valorisation* (pp. 171-204). Cham: Springer Nature Switzerland.

McCurry, M. O. (1985). Petrology of the Woods Mountains volcanic center, San Bernardino County, California. California Univ., Los Angeles (USA).

NASRDA - Department of Strategic Space Application, National Space Research and Development Agency, (2018). Benefits of Nigeria Satellite.

Nataraj, S. K. (2024). *Materials and Methods for Industrial Wastewater and Groundwater Treatment*. John Wiley & Sons.

NGSA (Nigeria Geological Survey Agency) 2011. Geological map of Abuja. Published by the Authority of the Federal Republic of Nigeria.

Oversby, V. M. (1975). Lead isotopic study of aplites from the Precambrian basement rocks near Ibadan, southwestern Nigeria. Earth and Planetary Science Letters, 27(2), 177-180.

Satheeshkumar, S. (2024). Assessment of groundwater potential using 1D model of vertical electrical sounding and aquifer protective capacity in the Naraiyur micro-watershed. *Modeling Earth Systems and Environment*, *10*(1), 913-925. DOI: https://doi.org/10.1007/s40808-023-01819-x

Servin Vega, F. L. (2024). *Thermal activation of tunnel infrastructures: insights from three Italian case studies* (Doctoral dissertation, Politecnico di Torino).

Sunkari, E. D., Kore, B. M., and Abioui, M. (2021). Hydrogeophysical appraisal of groundwater potential in the fractured basement aquifer of the federal capital territory, Abuja, Nigeria. Results in Geophysical Sciences, 5, 100012. https://doi.org/10.1016/j.ringps.2021.100012

Tanko, I. Y., Adam, M., and Dambring, P. D. (2015). Field features and mode of emplacement of pegmatites of Keffi area, north central Nigeria. International Journal of Scientific & Technology Research, 4, 214-229.

Udosen, N. I., Ekanem, A. M., & George, N. J. (2024). Geophysical exploration to assess leachate percolation and aquifer protectivity within hydrogeological units at a major open dump in Eket, Nigeria. Results in Earth Sciences, 2, 100022. DOI: https://doi.org/10.1016/j.rines.2024.100022

Wei, Y., Chen, Y., Cao, X., Xiang, M., Huang, Y., & Li, H. (2024). A critical review of groundwater table fluctuation: formation, effects on multifields, and contaminant behaviors in a soil and aquifer system. *Environmental Science & Technology*, *58*(5), 2185-2203.

Disclaimer (Artificial intelligence)

Option 1:

Author(s) hereby declare that NO generative AI technologies such as Large Language Models (ChatGPT, COPILOT, etc.) and text-to-image generators have been used during the writing or editing of this manuscript.